From ductile to brittle: Evolution and localization of deformation below a crustal detachment (Tinos, Cyclades, Greece)

C. Mehl, L. Jolivet, and O. Lacombe

Laboratoire de Tectonique, UMR 7072, Université Pierre et Marie Curie, Paris, France

Received 9 November 2004; revised 15 March 2005; accepted 9 May 2005; published 27 August 2005.

[1] The Cycladic Oligo-Miocene detachment of Tinos island is an example of a flat-lying extensional shear zone evolving into a low-angle brittle detachment. A clear continuum of extensional strain from ductile to brittle regime is observed in the footwall. The main brittle structures marking extension are shallow- and steeply dipping normal faults associated with subvertical extensional joints and veins. The earliest brittle structures are low-angle normal faults which commonly superimpose on, and reactivate, earlier (precursory) ductile shear bands, but newly formed low-angle normal faults could also be observed. Low-angle normal faults are cut by late steeply dipping normal faults. The inversion of fault slip data collected within, and away from, the main detachment zone shows that the direction of the minimum stress axis is strictly parallel to the NE-SW stretching lineation and that the maximum principal stress axis remained subvertical during the whole brittle evolution, in agreement with the subvertical attitude of veins throughout the island. The high angle of σ_1 to the main detachment suggests that the detachment was weak. This observation, together with the presence of a thick layer of cataclasites below the main detachment and the kinematic continuum from ductile to brittle, leads us to propose a kinematic model for the formation of the detachment. Boudinage at the crustal scale induces formation, near the brittle-ductile transition, of ductile shear zones near the edges of boudins. Shear zones are progressively exhumed and replaced by shallow-dipping cataclastic shear zones when they reached the brittle field. Most of the displacement is achieved through cataclastic flow in the upper crust and only the last increment of strain gives rise to the formation of brittle faults. The formation of the low-angle brittle detachment is thus "prepared" by the ductile shear zone and the cataclasites and favored by the circulation of surface-derived fluids in the shear zone. **Citation:** Mehl, C., L. Jolivet, and O. Lacombe (2005), From ductile to brittle: Evolution and localization of deformation below a crustal detachment (Tinos, Cyclades, Greece), *Tectonics*, *24*, TC4017, doi:10.1029/2004TC001767.

0278-7407/05/2004TC001767$12.00

1. Introduction

[2] Postorogenic extension has been the subject of numerous studies during the last 30 years. Direct field observations in several regions such as the Basin and Range Province or the Aegean Sea [*Crittenden et al.*, 1980; *Wernicke*, 1981; *Miller et al.*, 1983; *Coney and Harms*, 1984; *Lister et al.*, 1984; *Lister and Davis*, 1989; *Wernicke*, 1992; *Gautier et al.*, 1993; *Gautier and Brun*, 1994a; *Jolivet et al.*, 1994; *Wernicke*, 1995; *Jolivet and Patriat*, 1999; *Sorel*, 2000], as well as seismological studies [*Rigo et al.*, 1996; *Sachpazi et al.*, 2003] have provided constraints on the geometry and kinematics of extensional structures. It is now admitted that the continental crust extends by normal, steeply or shallow-dipping faults in its upper brittle part [*Jackson*, 1987; *Jackson and White*, 1989] and by kilometer-scale shear bands in the brittle-ductile transition and more distributed deformation in its lower part. Within metamorphic core complexes, brittle and ductile structures are separated by low-angle normal faults, or detachments, initially recognized in the Basin and Range Province [*Davis and Coney*, 1979; *Crittenden et al.*, 1980; *Wernicke*, 1981; *Davis and Lister*, 1988] and first described in the Aegean Region in Naxos [*Lister et al.*, 1984]. Detachments are interpreted as the final evolution of shear bands toward a more localized deformation [*Lister and Davis*, 1989]. The mechanism of shear localization within the brittle-ductile transition is, however, still poorly explained and several problems remain unexplained.

[3] First, how is it possible to localize deformation at the brittle-ductile transition where rheological profiles predict a maximum of resistance [*Brace and Kohlstedt*, 1980]? Three localizing factors reducing the deviatoric stress at the brittle-ductile transition are described in the literature: temperature, dynamic recrystallization and softening reactions. Temperature [*Kirby*, 1985] is most efficient at the base of the crust and cannot explain localization at the brittle-ductile transition. Grains are known to dynamically recrystallize only after relatively large strain [*Weathers et al.*, 1979]: therefore dynamic recrystallization may accelerate localization of deformation but cannot initiate the phenomenon. Numerous studies have put forward the role of softening reactions enhanced by fluid circulations in the localization of deformation below a detachment. One of the most often reported softening reaction consists of breakdown of relatively strong feldspars to easily deformable white micas [*Mitra*,

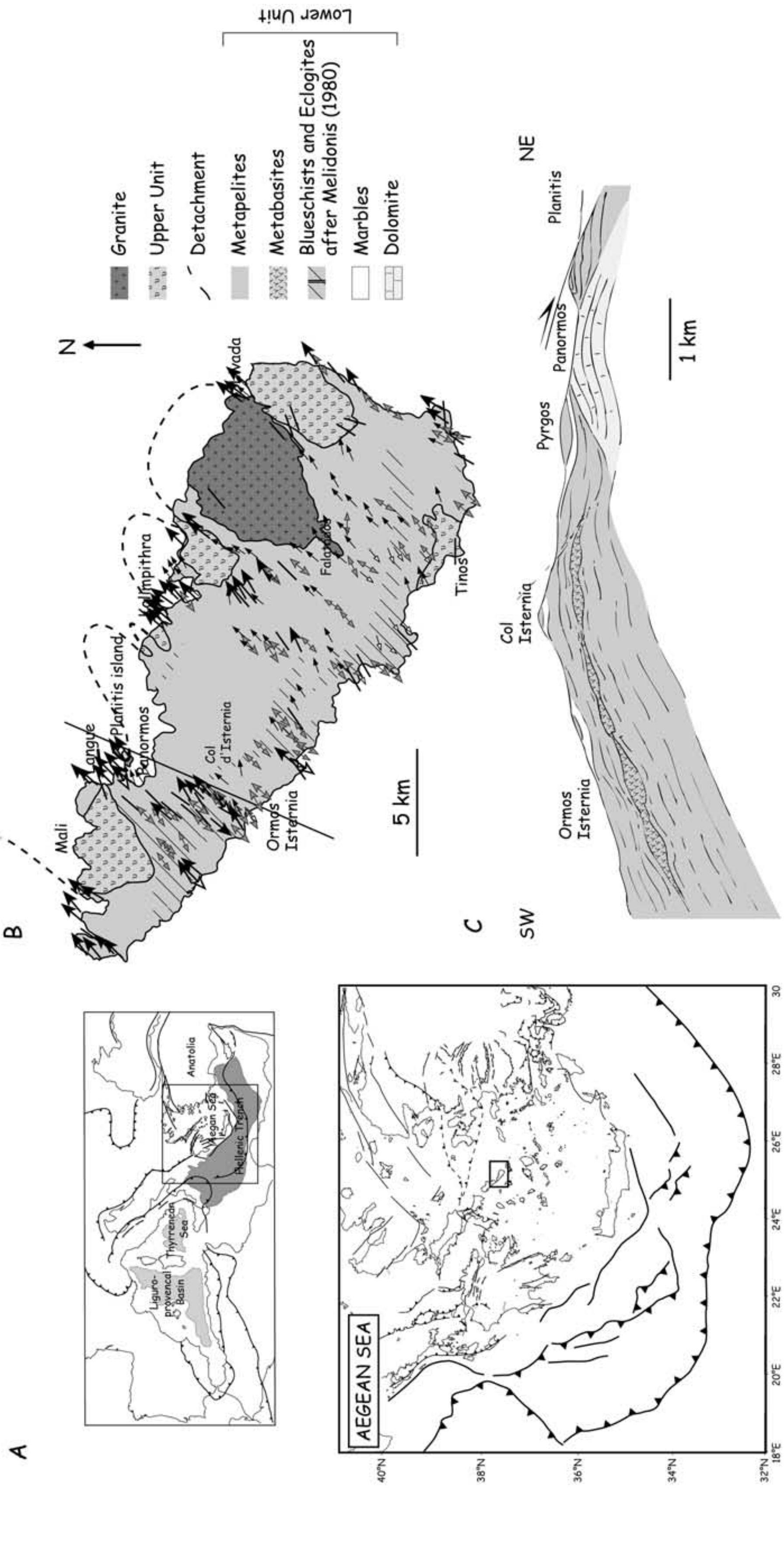
A
Liguro-provencal Basin
Tyrrhenean Sea
Anatolia
Aegean Sea
Hellenic Trench
AEGEAN SEA
B
N
Mali
Langue
Panormos
Planitis island
Kalimpithra
Vourvada
Falatados
Col d'Isternia
Ormos Isternia
Tinos
5 km
Granite
Upper Unit
Detachment
Metapelites
Metabasites
Blueschists and Eclogites after Melidonis (1980)
Marbles
Dolomite
Lower Unit
C
SW
NE
Ormos Isternia
Col Isternia
Pyrgos
Panormos
Planitis
1 km

Figure 1

1978; *White and Knipe*, 1978; *Dixon and Williams*, 1983; *Marquer et al.*, 1985; *Fitz Gerald and Stünitz*, 1993; *Wintsch et al.*, 1995; *Wibberly*, 1999; *Gueydan et al.*, 2001, 2003]. However, this reaction occurs in the late stage of deformation (greenschist facies), and consequently does not initiate localization. Moreover, in the Cycladic Blueschists where our study is located, the average concentration of micas does not change significantly during deformation, original rocks being already very rich in phyllosilicates.

[4] Second, how are brittle faults superimposed on previous ductile structures and why is the detachment so flat, in apparent contradiction to the classical laws of fault mechanics? This point is much debated. According to classical fracturing models, most authors argue for initially steeply dipping normal faults. Later flattening of the plane is explained by isostatic rebound or rotation generated by progressive increase of stretching [*Davis*, 1983] or later normal faults [*Buck*, 1988; *Wernicke and Axen*, 1988; *Block and Royden*, 1990; *King and Ellis*, 1990; *Wdowinski and Axen*, 1992; *Holm et al.*, 1993; *Sokoutis et al.*, 1993; *Brun et al.*, 1994; *Brun and Van Den Driessche*, 1994; *Gautier and Brun*, 1994a; *Gautier et al.*, 1999]. Some field, paleomagnetic and seismological evidence contradict this thesis and argue for an initially subhorizontal detachment [*Lister and Davis*, 1989; *Scott and Lister*, 1992; *John and Foster*, 1993; *Livaccari et al.*, 1993, 1995; *Rigo et al.*, 1996; *Jolivet and Patriat*, 1999; *Sorel*, 2000; *Flotté*, 2003; *Sachpazi et al.*, 2003]. A local reorientation of the tectonic stress field [*Spencer and Chase*, 1989; *Yin*, 1989; *Melosh*, 1990; *Wills and Buck*, 1997], a weak fault plane [*Jackson and White*, 1989] or the intervention of fluids are usually advocated to explain slip on a low-angle normal fault.

[5] In order to conceptualize a model taking into account the problems of the initial localization of ductile deformation and of the onset of brittle deformation onto ductile one, a complete and careful description of the succession of events that ultimately lead to localization of brittle faults is required. Tinos island in the Cyclades (Greece) provides an example of such a progressive localization and formation of an extensional detachment [*Gautier and Brun*, 1994a; *Jolivet and Patriat*, 1999]. The island, situated in the central part of the Aegean Sea, displays the characteristic structure of a metamorphic core complex. Two metamorphic units are superposed and separated by a sharp low-angle detachment. Rocks of the footwall were exhumed along the detachment. They progressively underwent and "froze" ductile and brittle deformation during their way back to the surface. *Jolivet et al.* [2004] propose, after preliminary field observations on the island, an additional localizing factor explaining the initial localization: rheological heterogeneities and boudinage. Boudinage first localizes deformation at intervals depending on the contrast of viscosity between strong and weak layers, then, extensional shear zones localize in the matrix at the ends or in the neck between boudins, as a consequence of a local increase of strain rate or of stress concentration. These shear zones ultimately evolve into faults, steep or shallow dipping.

[6] Several structural studies have been previously conducted in Tinos; some focused on the brittle deformation of the hanging wall and its consistency with the ductile deformation of the footwall [*Gautier and Brun*, 1994b; *Jolivet and Patriat*, 1999], while others emphasized the incoming of meteoric fluids during localization of deformation along the detachment [*Famin et al.*, 2004b]. Little attention has so far been paid, in the Aegean Sea, to the evolution from ductile toward brittle deformation within the footwall in the metamorphic core complexes. The two fold aim of this study is first to carefully describe the succession of small-scale structures from ductile shear bands to normal faults in the footwall of an extensional detachment and to discuss the continuum of strain during exhumation and the possibility of creating newly formed low-angle normal faults. We further aim at proposing a scheme of evolution of structures from ductile to brittle taking into account the development of shallow-dipping planes as well as a model of the tectonic evolution at the scale of the entire crust.

2. Geological Setting of Tinos Island

[7] Tinos is situated in the northern part of Cyclades (Figure 1a), in the back arc region of the Hellenic subduction, where crustal thinning has been active since the Early Miocene [*Le Pichon and Angelier*, 1981; *Jolivet and Faccenna*, 2000], leading to the formation of the Aegean Sea. Active extension is presently distributed around the Aegean Sea in west Turkey, in the Peloponnesus, in the Gulf of Corinth and in Crete [*Seyitoglu and Scott*, 1991; *Armijo et al.*, 1992, 1996; *Rietbrock et al.*, 1996; *Rigo et al.*, 1996; *Seyitoglu and Scott*, 1996] while the central part is more rigid. Present-day extension seems to be N-S oriented [*Le Pichon et al.*, 1995; *McClusky et al.*, 2000; *Jiménez-Munt et al.*, 2003]. Tinos displays a clear NW-SE elongated dome-shaped structure and shows a consistent NE trending stretching lineation [*Gautier and Brun*, 1994b; *Jolivet and Patriat*, 1999] (Figure 1b). Two tectonic units are superposed.

[8] 1. The upper unit consists of serpentinites, metagabbros and minor phyllitic rocks [*Melidonis*, 1980; *Avigad and Garfunkel*, 1989; *Bröcker*, 1990; *Patzak et al.*, 1994; *Katzir et al.*, 1996; *Stolz et al.*, 1997]. It was metamorphosed into the greenschist facies 70 Ma ago but has not been affected by the alpine high-pressure metamorphic event [*Avigad and Garfunkel*, 1989; *Katzir et al.*, 1996].

[9] 2. The lower unit is composed of metapelites, metabasites and marbles [*Melidonis*, 1980]. Though most rocks

Figure 1. (a) Location of Tinos island in a map of Aegean Sea, modified after *Jolivet et al.* [2004]. Tinos Island is situated on the northern part of the Cyclades, between the islands of Andros and Mykonos. (b) Geological map of Tinos Island, simplified after *Melidonis* [1980]. All outcrops studied in this work are located on the map. Lineations are reported on the map (data after *Gautier and Brun* [1994b], *Jolivet and Patriat* [1999], and this study). (c) Structural cross section of the island, simplified after *Famin* [2003].

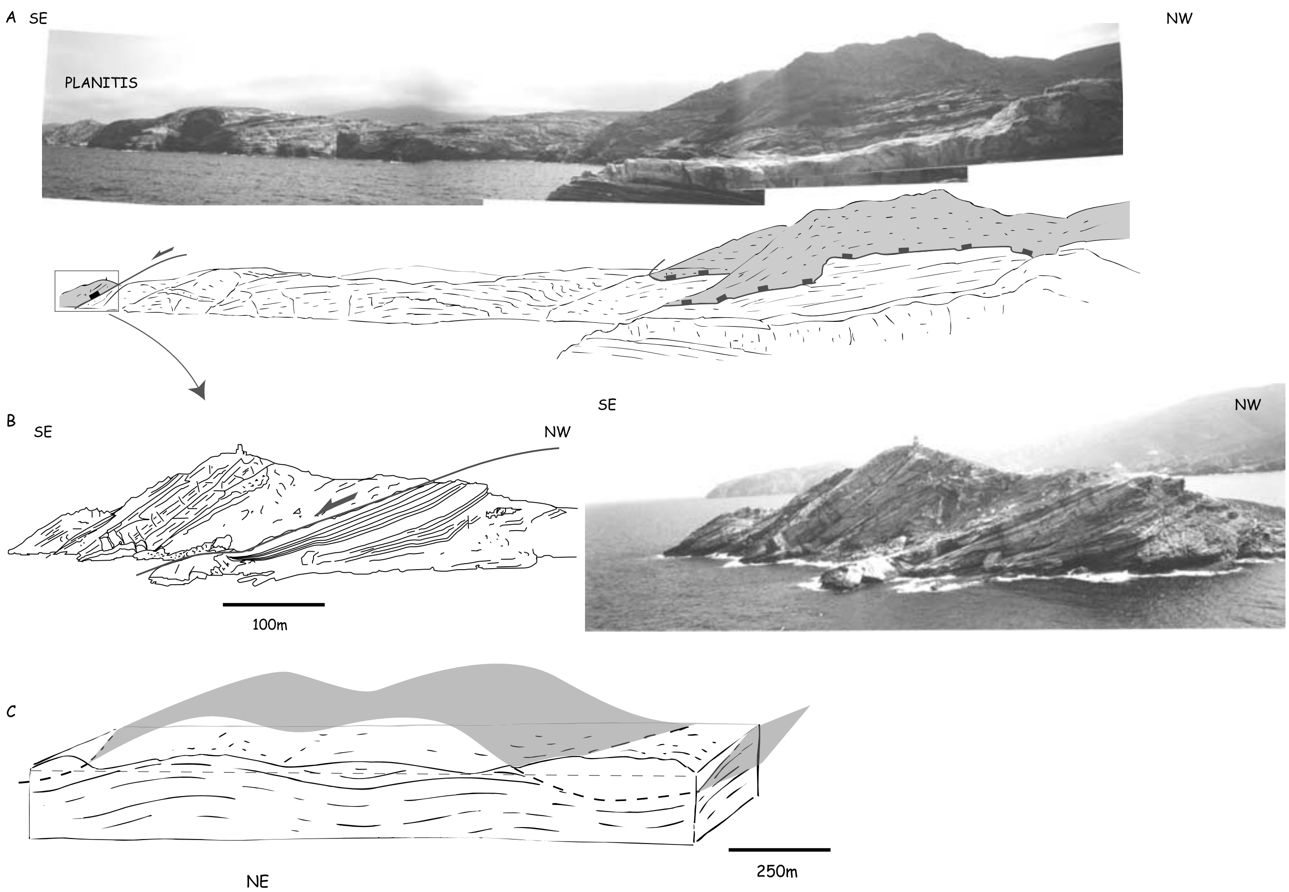

Figure 2. (a) View of the northern coast of the island. The outcrops of the Upper Unit are reported in grey. (b) Zoom of Planitis Island. The detachment corresponds to the grey plane. (c) Schematic sketch of the NE-SW folds affecting the foliation. Outcrops of the Upper Unit take place in the synclines. The detachment plane has been reported in grey.

of this unit display greenschist facies paragenesis, well-preserved eclogites and blueschists are exposed in the southwest half of the island [*Melidonis*, 1980; *Bröcker*, 1990; *Gautier and Brun*, 1994b; *Jolivet et al.*, 1998; *Jolivet and Patriat*, 1999]. Greenschist paragenesis formed preferentially along shear zones and are interpreted as synkinematic [*Gautier and Brun*, 1994b]. Fluids are involved in retrogression from blueschist toward greenschist facies [*Parra et al.*, 2002]. A conceptual scenario of fluids circulation related to the detachment has been proposed by *Famin et al.* [2004a, 2004b], based on structural interpretation of the different generations of veins, fluid inclusions and oxygen isotope analysis. This scenario puts forward the infiltration of meteoric fluids down to the brittle-ductile transition by transient enhancement of the permeability of the rocks at this transition.

[10] 3. Peak P-T conditions inferred for the high-pressure metamorphism are estimated at 15–18 kbar and 450–500°C [*Bröcker et al.*, 1993; *Parra et al.*, 2002]. Pressures and temperatures for the greenschist overprint are respectively estimated at about 7–4 kbar and 440–470°C [*Bröcker et al.*, 1993]. K-Ar, Ar-Ar, and Rb-Sr dating of white micas yielded ages between 55 and 40 Ma for blueschist facies and between 25 and 18 Ma for greenschist facies [*Altherr et al.*, 1982; *Bröcker et al.*, 1993; *Bröcker and Franz*, 1998]. A continuous record of retrograde P-T evolution coupled with published geochronological data demonstrate a three-stage exhumation history in Tinos [*Parra et al.*, 2002]: (1) a decompression from 18–15 kbar at 500°C to 9 kbar at 400°C, before ~37 Ma, with a cold path characteristic of synorogenic exhumation, (2) a thermal overprint from 400 to 500°C at around 9 kbar corresponding to thermal reequilibration without exhumation, possibly due to the transition in the stress regime between synorogenic and postorogenic extension around 30 Ma [*Jolivet and Faccenna*, 2000; *Parra et al.*, 2002], and (3) a decompression from 9 kbar at 550–570°C to 2 kbar at 420°C, taking place between 30 and 20 Ma, which is interpreted as a consequence of postorogenic extension. The question of a possible Miocene high-pressure event in the lower part of the complex has been raised by *Ring and Layer* [2003]. The basal unit in the whole Cyclades would have been buried in the subduction zone in the Early Miocene. *Bröcker et al.* [2004], however, discussed this hypothesis arguing that

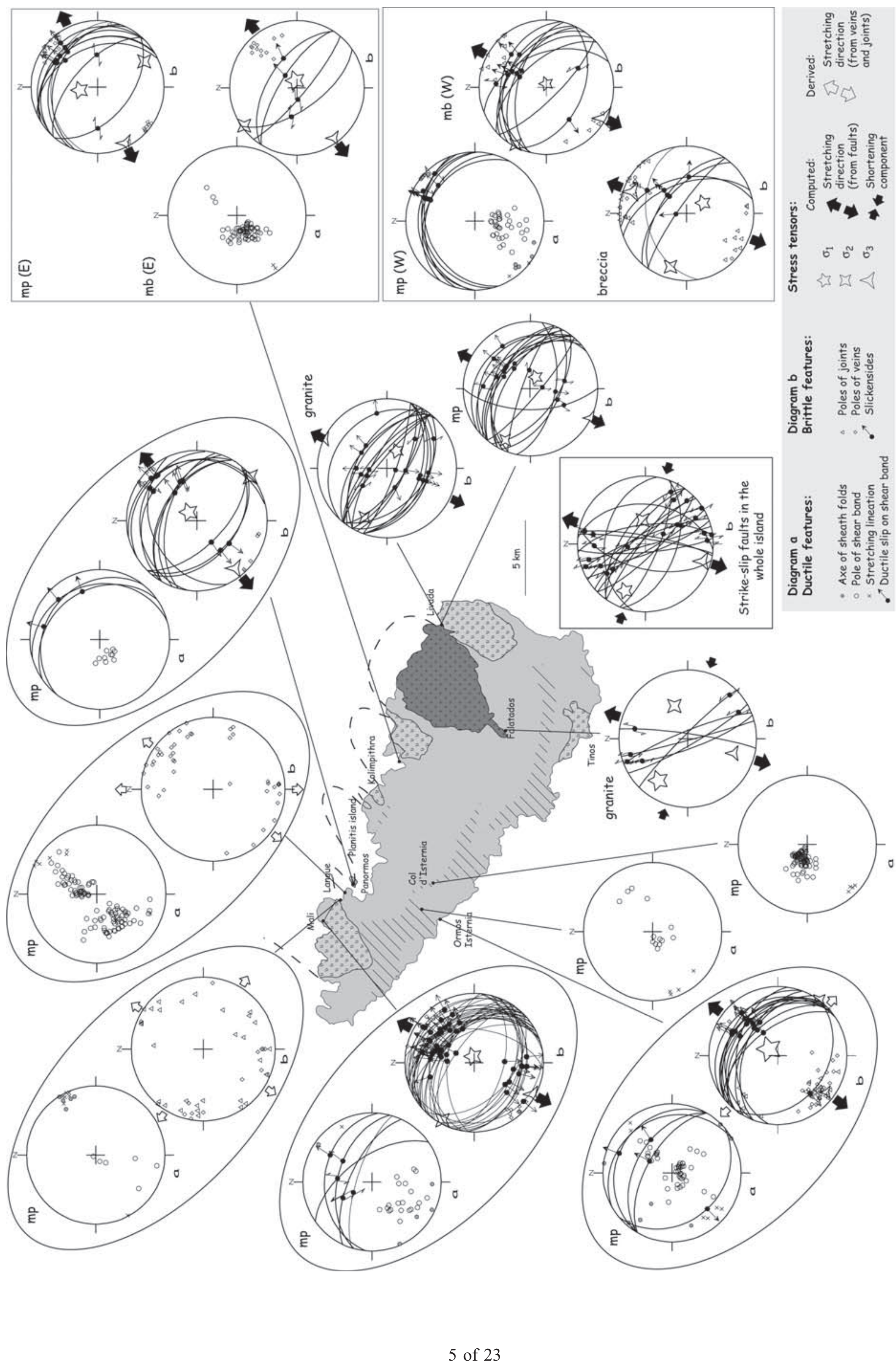
Livada
Falatados
Tinos
Kolimpithra
Planitis island
Panormos
Langue
Moli
Col d'Isternia
Ormos Isternia
5 km
mp
mb (E)
mp (E)
mb (W)
mp (W)
breccia
granite
Strike-slip faults in the whole island
Diagram a
Ductile features:
Axe of sheath folds
Pole of shear band
Stretching lineation
Ductile slip on shear band
Diagram b
Brittle features:
Poles of joints
Poles of veins
Slickensides
Stress tensors:
Computed:
Stretching direction (from faults)
Shortening component
Derived:
Stretching direction (from veins and joints)

Figure 3

ages around 20 Ma correspond to a resetting of phengites in the greenschist facies. This is well in line with the clear association of greenschist facies paragenesis with extensional shear zones in this part of the island [*Parra et al.*, 2002].

[11] A finite strain gradient is superimposed to the retrogression gradient, as seen on the cross section of the island (Figure 1c): the deformation evolves from coaxial flow in the southwest part of the island toward a noncoaxial flow with a top-to-the-northeast sense of shear in the domain of complete retrogression into the greenschist facies [*Jolivet and Patriat*, 1999]. A shallow NE dipping contact soled by a reddish breccia, i.e., the detachment, separates the two units on the NE side of the island. Some authors have recognized a third unit composed of a dolomite of Triassic age, cropping out in NW Tinos, below the blueschist unit [*Avigad and Garfunkel*, 1989]. A granodioritic pluton (14–19 Ma) intrudes both units and generates contact metamorphism. Since it cuts through the extensional ductile deformation and shows poor evidence of internal strain, it can be argued that the shear zone has progressively ceased to move during the intrusion [*Jolivet and Patriat*, 1999].

[12] During exhumation, rocks of the Lower Unit underwent ductile and brittle deformation. We aim at precisely describing small-scale ductile and brittle structures along a cross section from Ormos Isternia (SW side of Tinos) to Planitis (NE side, just below the detachment), in order to discuss the continuum of strain during exhumation and the way brittle structures are superimposed on ductile ones.

3. Field Evidence for a Continuum of Strain During Exhumation

3.1. Ductile Structures

[13] Tinos forms a NW-SE elongated dome structure with foliation flattening on the detachment, on the NE coast of the island. Some decameter-scale NE-SW folds affect the foliation [*Avigad et al.*, 2001]. They are observable on the northern coast of the island (Figure 2) and are consistent with a NW-SE component of ductile shortening.

[14] The lower unit of Tinos consists of a succession of metapelites, metabasites and marble layers. Metabasites under greenschist facies often form boudins within less competent metapelites. Fluid circulation seems to take place in the neck between boudins, where veins form consecutively to maximum extension. Rare sheath folds with NE-SW axes are preserved in the greenschists of the island, especially in Planitis and nearby where shearing is maximum. Boudins correspond to the earliest stage of localization under ductile behavior in the lower unit. We additionally observe an almost ubiquitous crenulation whose orientation is consistent with the component of perpendicular NW-SE shortening, already pointed out by the NE-SW fold axes.

[15] Numerous shear bands set on in the metapelitic matrix over the all island. Shear bands evolve from conjugate on the southwestern part of the island toward almost systematic NE dipping planes on the northeastern coast, in agreement with previous observations by *Jolivet and Patriat* [1999]. Because they concentrate deformation in narrow zones, they represent a higher degree of localization of deformation than boudins: they are thus interpreted to correspond to a later stage in the localization process. Their geometrical relation with boudins will be detailed in a later section.

[16] The direction of ductile extension was deduced from the attitude of stretching lineation, the projection of lineation on shear bands, and the axes of sheath folds (Figure 3). The data show a widespread consistent NE-SW direction of stretching.

3.2. Cataclasites

[17] The contact between the upper and the lower units is soled by several meter thick reddish breccia/cataclasites. Cataclasites have the same orientation and the same shallow dip as ductile shear bands. They accommodated stretching under ductile flow, but are affected by late brittle deformation (Figures 3 and 4): in the peninsula NW of Kolimpithra, the cataclasites show a clear reworking of the ductile foliation and stretching lineation by a high density of mineralized veins and subsequent brecciation and by late shallow-dipping faults. The presence of such small-scale faults cutting through the breccia/cataclasites suggests that they deformed under brittle behavior in the later stages of the exhumation and that movement along the cataclastic shear zone had probably nearly ended by then.

3.3. Veins

[18] Three generations of metamorphic veins have been described on the island. The first one (V_1) corresponds to synfolial quartz and calcite veins contemporaneous with the blueschist deformation and the onset of greenschist facies. The second generation (V2) is contemporaneous with greenschist deformation. The third generation of veins (V3) postdated the two others and developed under brittle conditions [*Famin et al.*, 2004b]. V_2 and V_3 have been used in this study to constrain deformation from the onset of localization under greenschist conditions to the late brittle stages of extension.

3.3.1. V2 Veins

[19] The SW limb of the dome shows systematically boudinaged V_2 veins (Figure 5a), embedded in a metapelitic matrix, such as in Ormos Isternia. Shear bands localize at

Figure 3. Schmidt's lower hemisphere equal-area projection of ductile and brittle structures studied on several outcrops of Tinos; mp, measurements made in metapelites; mb, measurements made in metabasites. Geological background is same key as in Figure 1. The a diagrams show ductile features. All features are consistent with a NE/SW extension during ductile deformation. NE dipping planes clearly outnumber the SW dipping ones. The b diagrams show brittle features. Note the good agreement between ductile and brittle extension.

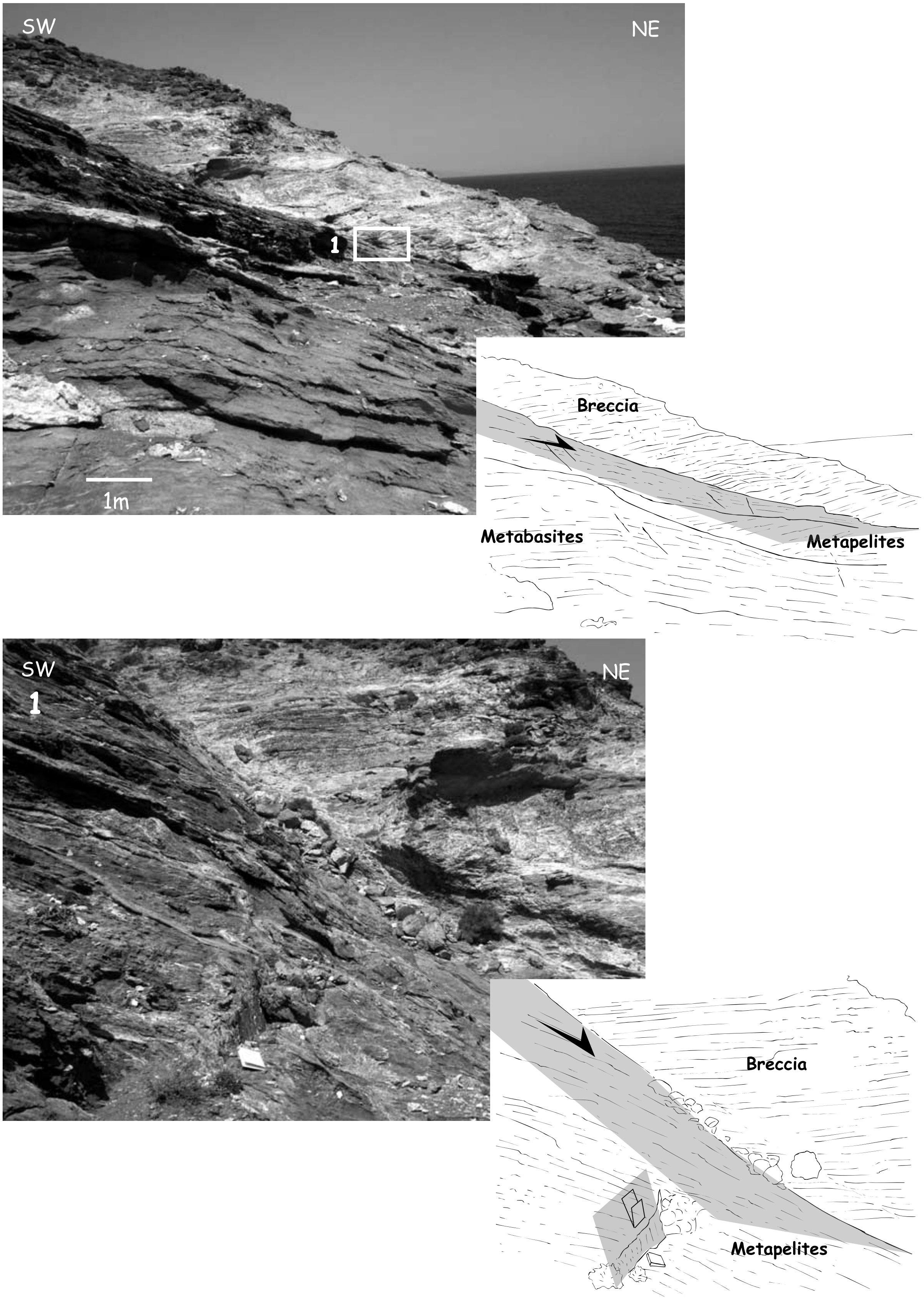
SW
NE
1
1m
Breccia
Metabasites
Metapelites
SW
NE
1
Breccia
Metapelites

Figure 4

the ends and in the necks between boudins. Conjugate shear bands are well represented: they dip toward SW as well as toward NE. A clear difference is seen with the veins on the NE side of the dome. Figures 5b and 5c are taken NW of Planitis and in Kolimpithra, respectively, on the northeastern coast of the island. Boudins deform here in an asymmetric manner. Shear bands always localize at the ends of boudins, but all planes dip toward NE. Low-angle fault planes of Figure 5c seem to be almost brittle.

[20] Boudinage is induced by the contrast of viscosity between the competent vein material and the relatively less competent metapelitic or metabasic matrix. Extensional shear zones often localize in the less competent matrix at the ends or in the neck between boudins, that is, in the zones of stress concentration. This observation supports that the initiation of shear bands postdated the boudinage of early veins, which is in good agreement with the fact and shear bands correspond to more localized deformation than boudins.

[21] As seen on Figures 5a–5c, boudins evolve from a symmetric shape on the SW coast toward asymmetric structures below the detachment. This evolution is related to the fact that NE dipping shear bands largely outnumber SW dipping planes when approaching the detachment. An evolution from coaxial toward noncoaxial flow with increasing strain could explain this asymmetry of ductile structures toward the detachment.

3.3.2. V3 Veins

[22] The third generation of veins corresponds to a late brittle increment of deformation of Tinos. It is composed of mixed sets of joints and veins at high angle to the foliation and cutting through the two other generations of veins. Measurements have been made on these V3 veins in Ormos Isternia, Mali, small headland NW of Panormos, Panormos, Planitis and Kolimpithra. Poles of veins are reported on Figure 3, b diagrams.

[23] The major part of these joints and veins indicates a widespread NE-SW direction of brittle extension (Figure 3). Some of them show a N-S direction of extension which may be related to the present extension in the Aegean (outcrops NW of Panormos, West Kolimpithra). Some veins of the outcrop of the small headland NW of Panormos and a few veins of Panormos additionally indicate a NW-SE component of extension which likely reflects a local accommodation of the main NE-SW extension.

[24] Most veins and joints are subvertical throughout the island and consistent with a nearly vertical shortening direction (within the 5° of uncertainties of measurements due to roughness of some planes). However, few joints and veins consistent with the NE-SW extensional trend are rather dipping 70–75° toward the SW or the NE, without any preference. Although the close association of these oblique sets with subvertical veins and the continuous range of dips from vertical to 70° could be simply related to natural dispersion, we tentatively propose that these sets could have opened as mixed mode I/mode II cracks/veins. The absence of fiber growth within the 70–75° dipping veins, however, precludes a direct confirmation of this inferred oblique opening.

3.4. Faults

[25] Several sites were recognized as demonstrative of the late structural evolution that accompanied the regional-scale extension during final cooling. Metapelites enclosing thin competent beds of metabasites allows observation of how normal faulting postdated boudinage in contrasted lithologies. Extensional microstructures evolved in type while the regional structure entered into the brittle domain, during synexhumation cooling. Normal faults developed in all lithologies, cutting through the foliation.

3.4.1. Overall Geometry of the Fault Network

[26] Structural analysis allowed the determination of the geometry of the fault network and the corresponding kinematics. Measurements of mesoscale fault planes were carried out in metapelites and metabasites (mp and mb, respectively, on Figure 3) for most sites, and in the granite for the outcrop of Livada (Figure 3), therefore covering a large range of lithologies. Results have been plotted on Figure 3, b diagrams.

[27] In Tinos, the most prominent fault sets cutting across the nappe pile trend NW–SE. Faults steepen in competent formations such as marbles and metabasites; they flatten, and are sometimes listric in metapelites. In all lithologies, displaced beds, veins, slickenfibers and other characteristic microstructures on fault planes, clearly document the dominant extensional nature of faulting. In some areas also, the normal faults are associated with left-lateral strike-slip faults, dominantly oriented NW-SE, kinematically consistent with normal faulting. Even if some striae indicate a N-S component of extension consistent with the present-day extension in the Aegean Sea, their small number and the difficulty to point out an univocal chronology have led us to rather consider a single major regional event of NE-SW extension. Note, however, that these faults are consistent with the few E-W trending subvertical veins previously described (outcrops NW of Panormos, West Kolimpithra).

[28] Diagrams show a wide range of dips for normal faults (between 5 and 85°): two kinds of faults can thus be distinguished in Tinos. Some of them are steeply dipping and correspond to "classical" features, others are shallow-dipping ones. The persistence of a continuous extensional stress regime during the development of the shallow and steeply dipping faults is suggested by the consistency of the pattern of fault strikes. Projection of faults shows that the NE shallow-dipping faults largely outnumber SW dipping ones. Only the site of Mali shows significant number of SW shallow-dipping conjugate faults. The question is: how do such brittle shallow and steeply dipping features initiate? A rigorous description and analysis is needed to propose a sketch of evolution of deformation.

Figure 4. Breccia at the contact between Lower and Upper Units in Kolimpithra. Breccia are affected by normal faults, which indicates their embrittlement during the last stages of exhumation.

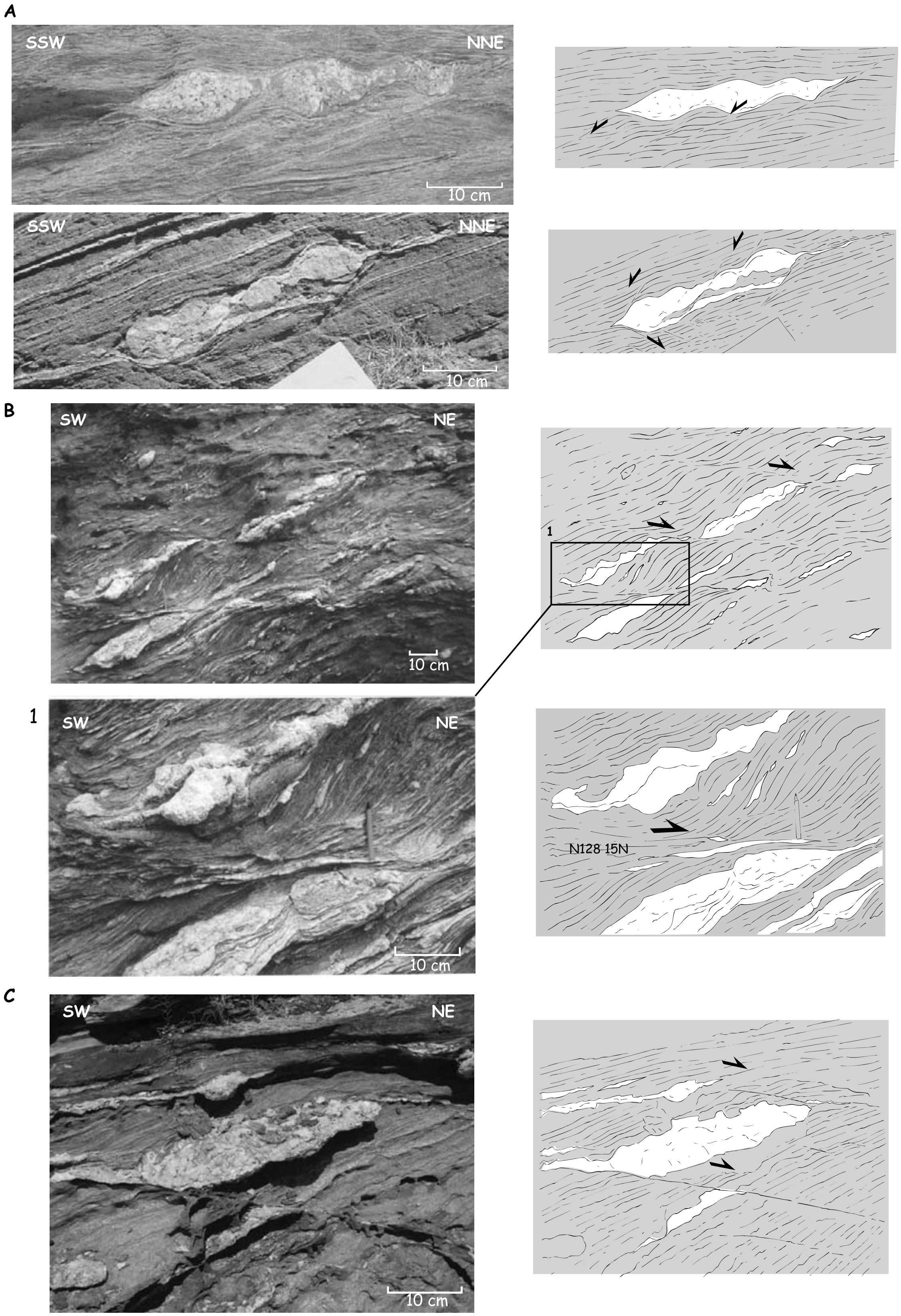
A
SSW
NNE
10 cm
SSW
NNE
10 cm
B
SW
NE
10 cm
1
1
SW
NE
10 cm
N128 15N
C
SW
NE
10 cm

Figure 5

3.4.2. Pattern of Shallow Dipping Faults and Association With Vertical Arrays of Veins

[29] Two kinds of shallow-dipping faults have to be distinguished in Tinos. The first one corresponds to shear bands that seem to have been reactivated in a brittle manner, or that have moved from ductile to brittle, the latest increment of deformation being discontinuous. Those features are well expressed in the area of Mali. Shistosity is bent on either side of the planes along which slickensides could sometimes be observed, indicating a discontinuous late increment of deformation in perfect kinematic agreement with ductile stretching lineation (Figure 6a). Such structures emphasize the continuum of kinematics between early ductile shearing and late discontinuous brittle slip. *Davis* [1983] as well as *Agard et al.* [2003] already reported such kinds of observations; Davis called the continuum of strain through time ''the kinematic coordination''. Some shallow-dipping faults form in the necks between asymmetric boudins (Figure 6b). Slip along these faults was sometimes accompanied by a component of dilatancy as indicated by their crystallized aspect. Associated veins presumably opened as little subvertical pull-aparts and clearly document the extensional nature of faulting (Figure 6b, boxes 1–3). Even if slickensides are not always observable, the shallow dip of the fault planes and their geometrical association with boudins lead us to conclude that they correspond to reactivated shear bands.

[30] The second kind of shallow-dipping faults initiated and moved exclusively in a brittle manner. These faults are well expressed in East Kolimpithra (Figure 7) and in Planitis (Figure 6). They are cutting across the ductile foliation and the late crenulation (Figures 6b and 7b). Their crosscutting relation with the late crenulation cleavage and folds shows that they are not controlled by any preexisting planar anisotropy such as a ductile shear band. The presence of conjugate SW shallow-dipping faults in Mali and Planitis confirms the fact that some low-angle planes are newly formed. Mali and Planitis are situated just below the detachment, where no SW dipping shear bands are recorded. In this place, SW shallow-dipping planes cannot be explained by the reactivation of preexisting shear bands. These faults are commonly associated with arrays of vertical veins. For example, Figure 7a shows shallow-dipping normal faults and contemporaneous vertical veins induced by the extensional regime in the hanging wall of the faults. Such structures are similar to those well documented for strike-slip faults, with a contraction zone characterized by pressure solution on one side of the plane and an extensional zone marked by veins on the other side [*Crider and Peacock*, 2004]. The close association between shallow-dipping normal fault planes and vertical veins is also illustrated by Figure 7b. Some vertical veins cut across shallow planes, some others are crosscut by the planes: vertical veins and shallow-dipping normal faults are thus coeval. Shallow-dipping ''newly formed'' faults seem to have been initiated under a vertical compressional direction, in contradiction with the classical laws of fault mechanics. The question of the mechanics of initiation of such faults will be discussed in further sections.

[31] Newly formed low-angle planes cut across ductile shear bands, but no criterion has been found to constrain the chronology between reactivation of shear bands and initiation of new shallow-dipping planes. ''Reactivation'' should be understood here as a continuum of shear from ductile to brittle with an increasing localization within a precursory shear band. In contrast, initiation of new shallow-dipping planes corresponds to a pure brittle deformation: we thus assume that initiation of new fault planes occurs after, or contemporaneous with, the last increment of motion along preexisting shear bands.

[32] In summary, we can conclude the following:

[33] 1. Two kinds of shallow-dipping faults are then distinguished. The first ones, as seen in Planitis (Figure 6b), are closely associated with lithological heterogeneities and boudins. They have attitudes and dips similar to those of ductile shear bands already described in section 3.1. They may therefore have formed by the ''reactivation'' of preexisting planar anisotropies, like shear bands and may have propagated into the matrix. The second ones, as seen in East Kolimpithra (Figure 7b), form in the absence of any boudins and cut across the ductile foliation. Consequently, they did not form by reactivation but rather as ''newly formed'' fractures.

[34] 2. The association of two kinds of shallow-dipping planes with vertical veins supports that the compression axis was a priori vertical during their formation.

[35] 3. Shallow-dipping faults are more numerous in metapelites than in metabasites, i.e., in weaker lithologies, especially due to the high mica content. Faults dipping toward NE are the most frequent, but conjugate faults dipping shallowly toward SW also occur (Figure 3).

3.4.3. Pattern of Steeply Dipping Faults

[36] The metapelites of Mali (Figure 8a) present a succession of shear bands making a progressively larger angle with the foliation. The final step of evolution corresponds to steeply dipping, often ''dilatant'' normal fault planes.

[37] In East Kolimpithra and Mali, metapelites present characteristic steeply dipping meter-scale fault planes with well-expressed conjugate patterns. Displaced beds (Figure 8b) and microstructures on fault planes (Figure 8c) document the extension. Note, on the left side of picture 8c, a boudinaged synfolial vein which has been folded and crosscut by a NE steeply dipping normal fault. Steeply dipping normal faults are sometimes associated with small-

Figure 5. Ductile structures illustrating that rheological inhomogeneities may be an efficient localizing factor of ductile simple shear deformation. (a) Two symmetric boudins in Ormos Isternia (southern coast of the island). Shear bands localize at the ends or in the necks between boudins. (b) Evolution toward asymmetric boudins near Panormos, on the northern coast of the island. Shear bands localize at the end of boudins. They all dip toward NE. (c) Shallow dipping planes localizing at the ends of boudins in Kolimpithra. The NE dipping planes seem here more brittle than the shear bands already described.

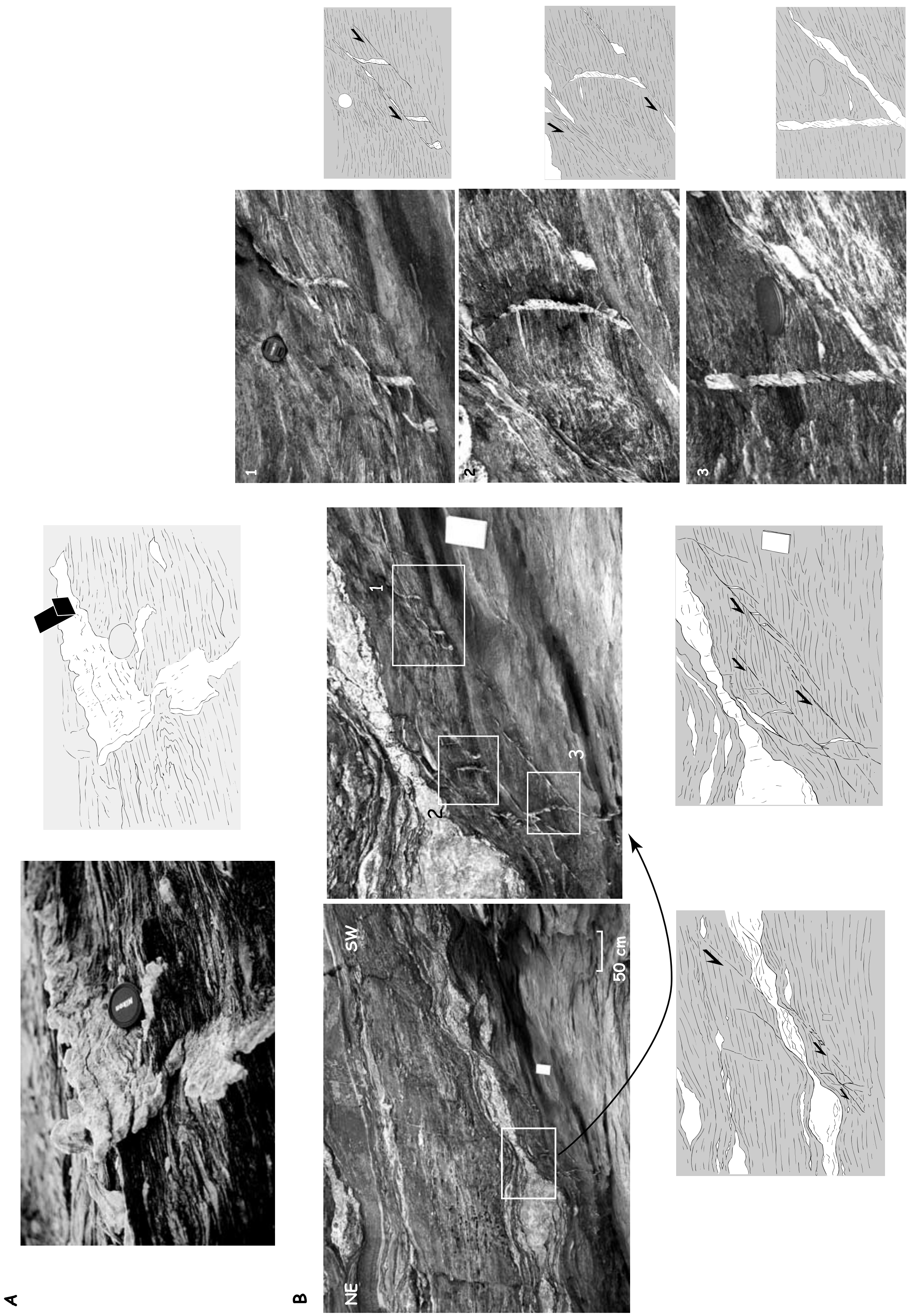

Figure 6

scale pull-aparts at extensional relays. In Livada (Figure 8d) decameter-scale steeply dipping planes are observable in metapelites. They flatten above shallow-dipping planes.

[38] In West Kolimpithra (Figures 9a and 9b), the chronology between shallow and steeply dipping faults is illustrated at different scales. Steeply dipping faults always cut across the new shallow-dipping ones, and therefore correspond to the final stage of localization.

[39] In summary, the following conclusions can be made:

[40] 1. Steeply dipping faults well illustrate the setting of brittle structures by progressive steepening during evolution from ductile to brittle behavior: the larger the angle, the more brittle the deformation. Steeply dipping faults always postdate shallow-dipping faults and are interpreted as newly formed faults marking the latest stage of brittle deformation.

[41] 2. In Tinos, brittle structures evolve from rather asymmetric with a majority of NE early shallow-dipping planes, toward the more symmetric pattern of the late steeply dipping faults. This suggests an evolution of deformation in the footwall of the detachment from noncoaxial stretching in the early stages of deformation to a more coaxial extension during the later stages of exhumation of the footwall. The overall component of simple shear presumably decreases with time during exhumation and ductile to brittle transition while simple shear tends to localize with time on a single fault plane, the detachment itself.

3.5. Conclusions

[42] The coaxiality of ductile and brittle extension, the fact that crenulation of ductile structures is consistent with the strike-slip component of faulting, and the consistency between ductile lineation and markers of extensional slip on fault planes lead us to conclude to a continuum of strain during exhumation. The second part of this study, having described ductile and brittle structures on the island, consists in explaining how ductile structures progressively localize and the way brittle normal structures are superimposed on ductile ones.

4. Interpretation of Field Data: Development of Ductile and Brittle Structures During Localization of Deformation

4.1. Boudinage, the First Localizing Factor of Ductile Deformation

[43] As already pointed out in the description of ductile structures, shear zones almost systematically localize at the end or in the neck of boudins. Such close association of structures has led *Jolivet et al.* [2004] to conclude that rheological heterogeneities and boudinage have to be considered as an efficient factor to initiate localization. The authors propose a scenario of evolution of early localization of deformation: first, boudinage localizes deformation at intervals depending on the contrast of viscosity between strong and weak layers and of the thickness of the competent layer. Then, it induces local increase of strain rate and/or stress concentration at the end or in the neck between boudins. The higher strain rate allows development of extensional shear zones in the matrix at the ends or in the neck between boudins. The authors interpret the overall structure of the islands in the same way, the dome being a 10-km-wide boudin limited to the northeast by the main detachment. The importance of crustal-scale boudinage was proposed in the early papers describing Metamorphic Core Complexes in the Basin and Range Province. *Davis and Coney* [1979], *Davis* [1980, 1983], and *Davis and Hardy* [1981] introduced the concept of megaboudinage at the scale of the MCC. The upward arching of the core rocks and of the decollement between the core and the cover were interpreted in terms of boudinage of two layers with contrasted rheologies separated by a decollement zone. The concept proposed by *Jolivet et al.* [2004] and developed in the present paper clearly derives from these early papers but it contains specific new points. First of all, crustal-scale boudinage in the Aegean is clearly asymmetric and the decollement does not correspond to a reactivated core-cover interface but rather to a new shear zone initially oblique to the main lithological interface (to explain the contrast in peak metamorphism). Second we emphasize the role played by boudinage to concentrate stress and strain and to induce the formation of localized shear zones and ultimately faults between boudins when crossing the ductile to brittle transition zone.

4.2. Development of Brittle Extensional Structures

[44] Two kinds of normal faults have been pointed out in the previous section of this work: steeply dipping faults displaying symmetric conjugate patterns and more asymmetric shallow-dipping faults. Steeply dipping faults newly form and clearly postdate shallow-dipping ones: they clearly develop in the last stage of localization of deformation. The onset of shallow-dipping planes is more complex. Some of them were presumably created by reactivation of preexisting planar anisotropies (shear bands) while others clearly initiated and propagated through the metamorphic pile without superposing on any preexisting planar anisotropy. The second ones are contemporaneous with vertical veins, which supports that they form a priori under a vertical attitude of the maximal principal stress axis. This a priori

Figure 6. (a) Slickensides on a fault plane in Mali. Crystallizations give a slip vector which is perfectly consistent with the ductile lineation observable on the left side of the picture: such a feature illustrates the continuum of strain between ductile and brittle structures. (b) Brittle shallow-dipping planes localizing between the necks or at the ends of boudins. These planes develop at the same place and have the same dip than shear bands. Their rheology is clearly brittle, with the opening of pull-apart type veins between two consecutive planes (A1, A2, A3). Fibers in veins are consistent with the direction of slip along the planes (A2, A3). The similarities between their position and dip with those of shear bands led us to conclude that such structures form on preexisting planar anisotropies.

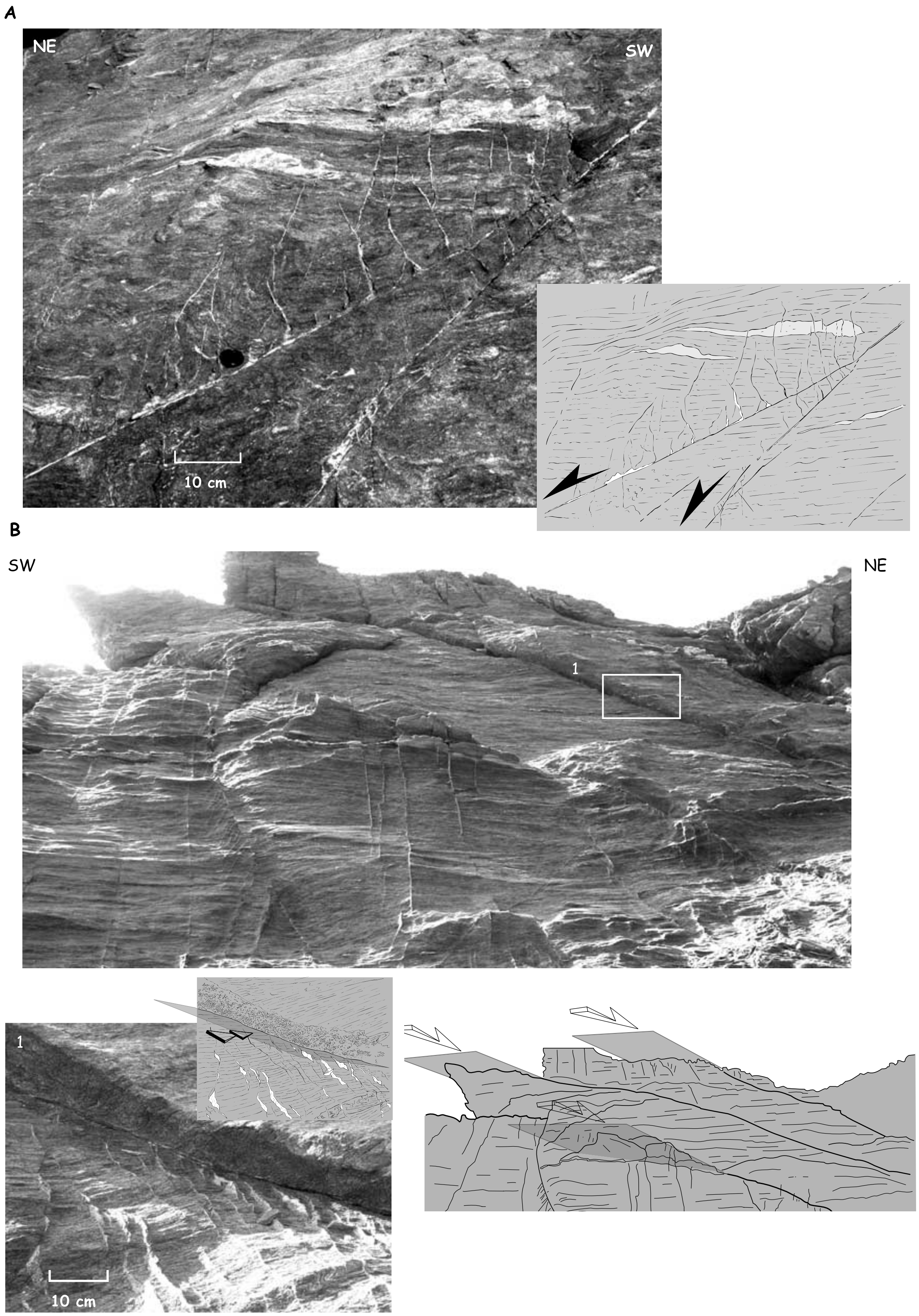

Figure 7

vertical position of the compressive stress axis is elsewhere confirmed by the presence of dacitic dikes on the island, that are assumed to have intruded as vertical sheets and are still vertical [*Avigad et al.*, 1998]. In this section, we will try to discuss mechanical problems inferred from the development of these steeply and shallow-dipping planes.

4.2.1. Initiation of Normal Faults by Reactivation of Preexisting Planar Anisotropies

[45] Onset of shallow-dipping normal faults, even under a vertical compression axis, considering reactivation of preexisting weaknesses does not constitute a real mechanical problem. *Reynolds and Lister* [1987] and *Axen and Selverstone* [1994] already argued for a vertical maximum stress axis around low-angle normal faults in metamorphic core complexes. *Axen and Selverstone* [1994] proposed a mechanical analysis of the Whipple detachment fault. They measured angles between steeply dipping, shallow-dipping faults and σ_1 and deduced from calculation using Mohr diagrams, assuming that the detachment was a preexisting weakness with no cohesive strength, that shallow-dipping faults could slip under moderate fluid pressure and relatively high differential stress if the zone surrounding the faults has a significant cohesion and fails in transtension.

[46] We propose that some shallow-dipping faults can be considered as having developed with precursory structures such as ductile shear zones, following that in the work by *Crider and Peacock* [2004]. However, shear bands do not consist of surfaces of displacement discontinuity; they are not themselves, strictly speaking, faults. So the term "reactivation", commonly understood as sliding along a preexisting discontinuity, should be considered with care. In fact, by "reactivation" we mean herein that discontinuous brittle slip is "prepared" by ultime localization of shear within a precursory shear band, within a clear kinematic continuum.

[47] "Reactivation" of some earlier shear bands could explain the larger number of NE dipping shallow planes. This asymmetry could be induced by the preexisting asymmetry of ductile shear bands: NE dipping shear bands are more represented than SW dipping ones, especially when approaching the detachment, due to a component of noncoaxial flow during ductile deformation. The very high mica content of metapelites which therefore display a low friction angle could have favored slip along such shallow-dipping faults. Another way to explain the statistical asymmetry could be to consider a component of simple shear which could be efficient until the formation of shallow-dipping planes, but which probably remained limited as indicated by the nearly vertical attitude of $\sigma 1$ during deformation and occurrence of some conjugate faults. This hypothesis will be discussed in the further section.

4.2.2. New Formation of Normal Faults in Tinos and Andersonian's Mechanics: Insights From Paleostress Reconstructions

[48] The mechanics of newly formed faults was developed in the 50s. According to the Coulomb failure criterion, *Anderson* [1951] predicted that newly formed normal faults should develop as conjugate fault patterns with opposite dips of comparable values and displaying vertical and horizontal planes of symmetry. Anderson concluded that the angle between two conjugate newly faults should be equal to 90° minus the angle of internal friction, generally 30° for most crustal rocks, so crustal extension is commonly accommodated by normal faults dipping 60°. *Jackson and White* [1989] statistically analyzed dip of nodal planes of the upper brittle part of the crust. They concluded the most common dip is in the range of 30–60° with a maximum around 50–55°.

[49] Andersonian's mechanics suitably explains the formation of the observed steeply dipping conjugate planes. During their way back to the surface, rocks undergo a decrease in temperature and pressure. They evolve toward a more competent rheology, that is, their angle of internal friction increased. The larger the friction angle, the smaller the angle between σ_1 and the fracturation plane. Therefore steeply dipping normal faults correspond to the expected evolution from ductile toward brittle. Brittle structures of Figure 8a illustrate this evolution. They do not contradict the laws of Andersonian's mechanics, and are otherwise consistent with the presence of contemporaneous vertical veins.

[50] In contrast, Andersonian's mechanics seems a priori to fail in explaining newly formed shallow-dipping planes. Even if considering a theoretical very weak material (supposed to deform, for example, under ductile conditions), with an angle of internal friction of 0°, the predicted maximum angle between maximum stress axis and fault plane is 45°. As a first approach we carried out inversion of fault slip data to deduce the orientation of principal stress axes and to verify their development under a nearly vertical σ_1 axis as suggested by the widespread vertical veins.

4.2.2.1. Principle and Aims of Reconstruction of Stress Regimes From Fault Slip Data in Tinos

[51] Many workers have applied the inversion method to derive regional paleostresses from fault slip data based on the Wallace-Bott hypothesis in many places worldwide during the last 30 years [e.g., *Letouzey*, 1986; *Bergerat*, 1987; *Mercier et al.*, 1989; *Angelier*, 1990] (see *Angelier* [1994] for further references). However, the theoretical suitability of the stress inversion method to derive principal stresses has been recently challenged by *Twiss and Unruh* [1998]. According to Twiss and Unruh, the deformation around a fault zone results from a slip discontinuity on the fault and can be modeled as an elastic deformation; in

Figure 7. (a) Shallow-dipping fault planes in Kolimpithra associated with vertical patterns of veins in the hanging wall. Verticality of veins associated with faults a priori indicates that shallow-dipping faults created in relation to a vertical compression axis. (b) Three meter-scale shallow-dipping normal faults in Kolimpithra East. Detailed picture shows that planes clearly cut across the foliation: no reactivation of preexisting shear bands can be advocated to explain nucleation of these faults. They are likely newly formed. Note that they are associated with vertical veins.

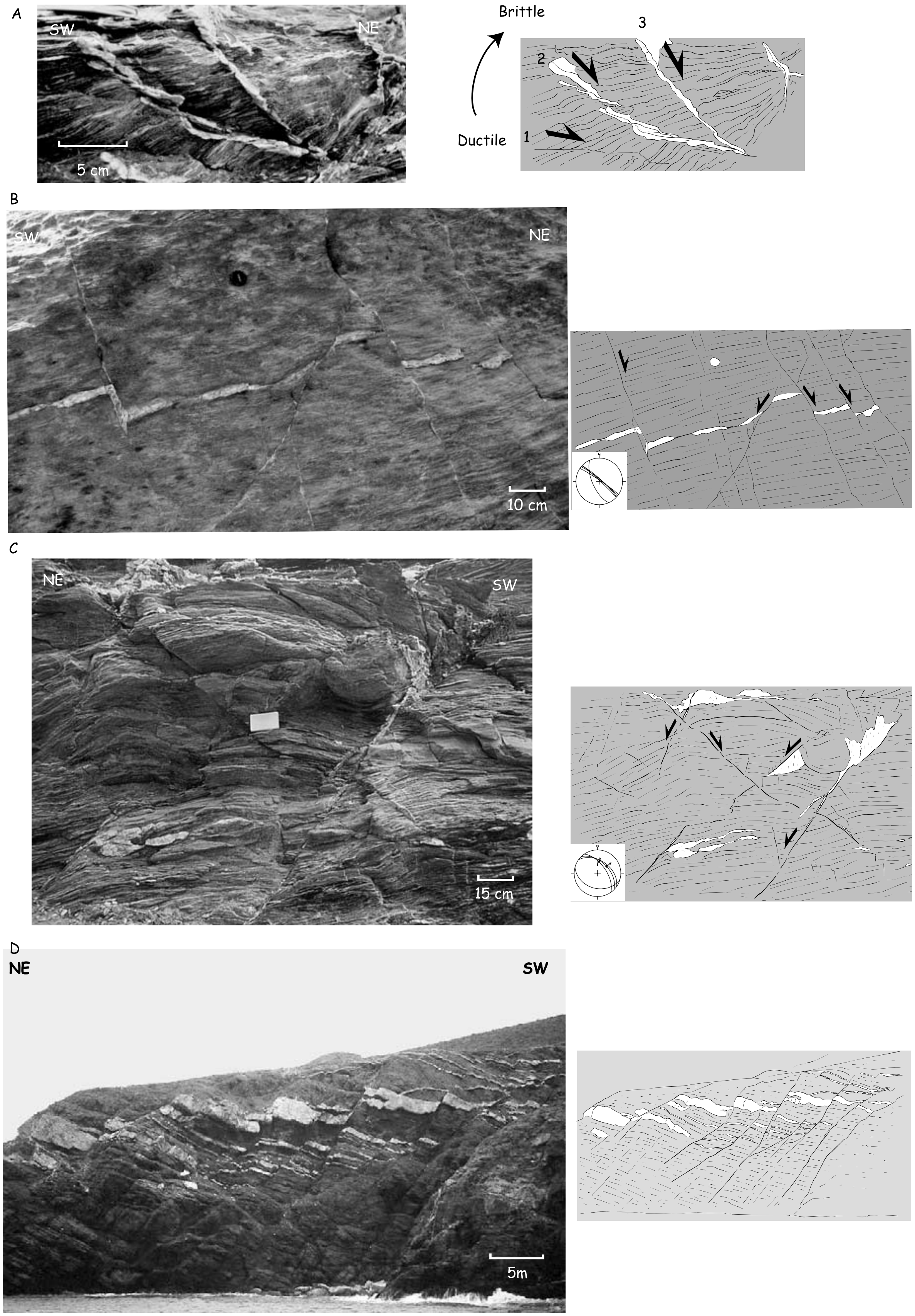
A
SW
NE
5 cm
Brittle
Ductile
1
2
3
B
SW
NE
10 cm
C
NE
SW
15 cm
D
NE
SW
5m

Figure 8

contrast, within the fault zone, the deformation results from a multitude of brittle slip events smoothed over the volume of the fault zone and is better described in terms of cataclastic flow. In addition, fault zones are known to be often associated with a strong rheological and/or mechanical anisotropy, important displacements and large noncoaxial deformation, so the local stress field is presumably inhomogeneous in both orientation and magnitude and could be not representative of the far-field stress of interest. Within fault zones, a kinematic interpretation of fault slip data in terms of strain rate seems theoretically more appropriate than the interpretation in terms of stress, because accurately deriving stress would require both an isotropic rock material and a linear constitutive relationship between stress and strain rate for cataclastic flow which is at the present state of our knowledge not established.

[52] Our fault slip data were collected on late, outcrop-scale faults displaying small offsets and a large scatter in attitudes and cutting through the ductile rock fabrics (foliation and shear bands). Thus, for the sites located away from the major detachment, i.e., the fault zone, paleostress reconstructions reported in this paper fulfill the assumptions of stress homogeneity and low finite strain which can be approximated by nearly coaxial conditions and therefore likely yield the regional paleostresses of interest. The a posteriori consistency of the stress regimes derived from both the inversion of striated faults and the statistical analysis of patterns of veins, from one site to another, in spite of significant lithological variations (metabasites, metapelites, granite) will support the reliability of the results of the performed study. The first aim of our stress analysis was therefore to derive the orientation of the maximum principal stress $\sigma 1$ which will be compared to the attitude of veins and will allow discussion of the suitability of Andersonian mechanics in explaining normal faults in Tinos.

[53] The second goal was to compare the stress regimes in sites away and closer to the detachment, including in the cataclasites below the detachment. If the stress regimes are found homogeneous throughout the whole island whatever the distance to the detachment, including in the fault zone itself, this will indicate that the late small-scale brittle faults developed in relation to the regional far-field stress and therefore that cataclastic flow within the extensional shear zone was probably no longer efficient during the last brittle increment of extensional strain; it will further indicate that cataclasites have progressively embrittled during exhumation.

[54] For these aims, stress tensors were calculated using the direct analytical inversion method [*Angelier*, 1990]. Inversion is based on the stress hypothesis, i.e., the assumption that the slip direction on any given fault plane is parallel to the direction of shear stress induced on this plane by an homogeneous stress tensor [*Wallace*, 1951; *Bott*, 1959]. Orientation and dip of faults, as well as direction and sense of slip are required to carry out inversion. A reduced stress tensor is obtained, that is the orientation of the principal stress axes σ_1, σ_2 and σ_3 ($\sigma_1 \geq \sigma_2 \geq \sigma_3$, compression positive) and a scalar invariant ϕ characterizing the shape of the stress ellipsoid.

$$\Phi = (\sigma_2 - \sigma_3)/(\sigma_1 - \sigma_3), \ 0 \leq \phi \leq 1$$

Inversion minimizes the misfit of the predicted shear and observed slip within the fault plane. Where the stress axes are computed from well defined conjugate fault sets as in most sites in Tinos (Figure 3), the uncertainties on their orientation remain lower than 10°. The good agreement between the stress axes computed from striated faults and the orientation of veins measured in the same sites confirms that the results obtained are reliable and accurate.

4.2.2.2. Results of Fault Slip Inversion

[55] Brittle extensional structures (fault planes and slickenlines) have been systematically measured in different sites where they could be clearly identified. For all the sites illustrated in this paper, no data sorting was necessary and nearly all field measurements could be kept when computing a single tectonic regime. Results of inversion are presented on Figure 3. Principal stress axes have been plotted onto stereograms (Schmid's lower hemisphere equal area projection) summarizing the brittle features collected on the island. They confirm the subvertical orientation for the compression axis, in spite of the variations between lithologies. This subvertical orientation is consistent with the vertical patterns of veins often associated with normal faults and characterizes an extensional tectonic regime. The extension axis remains subhorizontal or gently dipping with a clearly defined NE-SW direction. The orientations of the computed stress axes are reported in Table 1, together with the values of the stress el1ipsoid shape ratio Φ and estimators of the quality of the numerical calculation of the tensor. The Φ values calculated on both shallow-dipping (partly inherited) and newly formed faults are in the range of 0.4–0.7, suggesting a generally well-defined homogeneous true triaxial extensional stress regime throughout the island.

Figure 8. Brittle newly formed steeply dipping faults. (a) Picture illustrating the onset of brittle deformation on steep planes. The shallow planes correspond to shear bands. (b) Newly formed steeply dipping faults in Kolimpithra. Displaced beds are consistent with normal slip along faults. Conjugate planes are well expressed. The diagram on the lower left-hand corner summarizes the fault network of the outcrop. (c) Steeply dipping planes in Mali. Conjugate planes are well expressed. Slickensides on faults unambiguously indicate normal slips. (d) Decameter-scale normal fault planes in the metapelites of Livada. Displacements of beds are consistent with normal slips along faults. Steeply dipping planes are associated with one shallow-dipping plane. Chronology is not clear here.

A

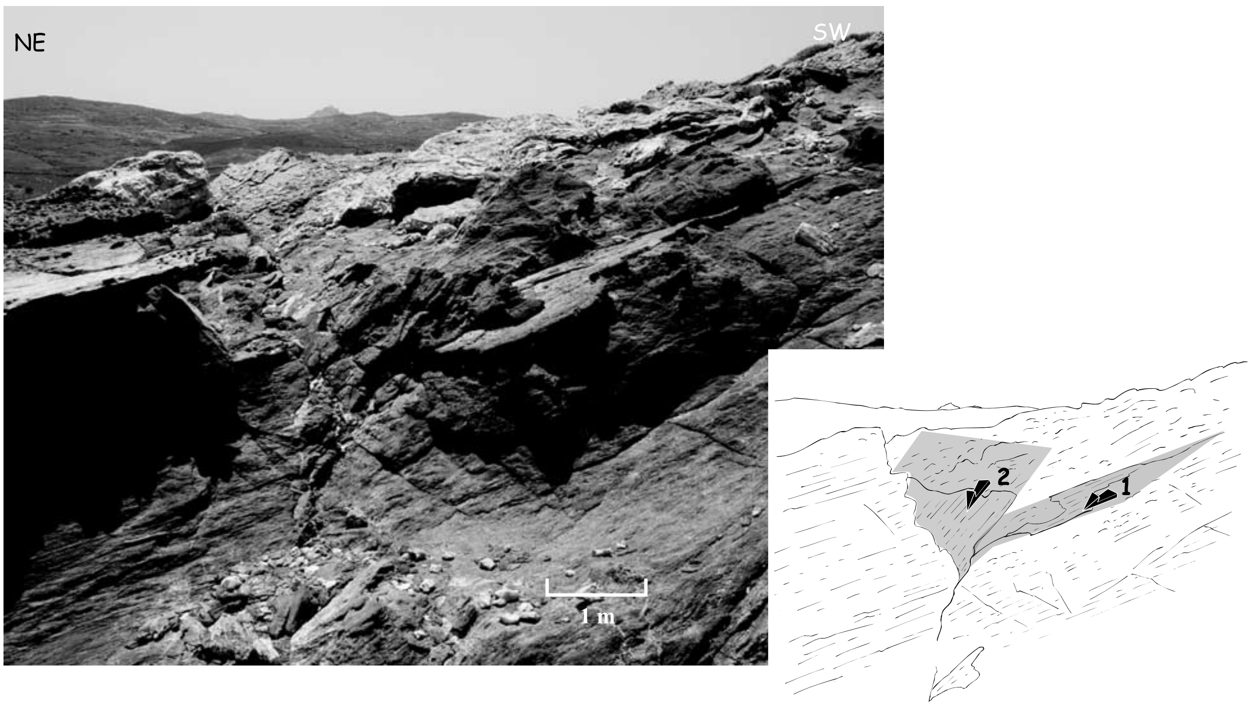

B

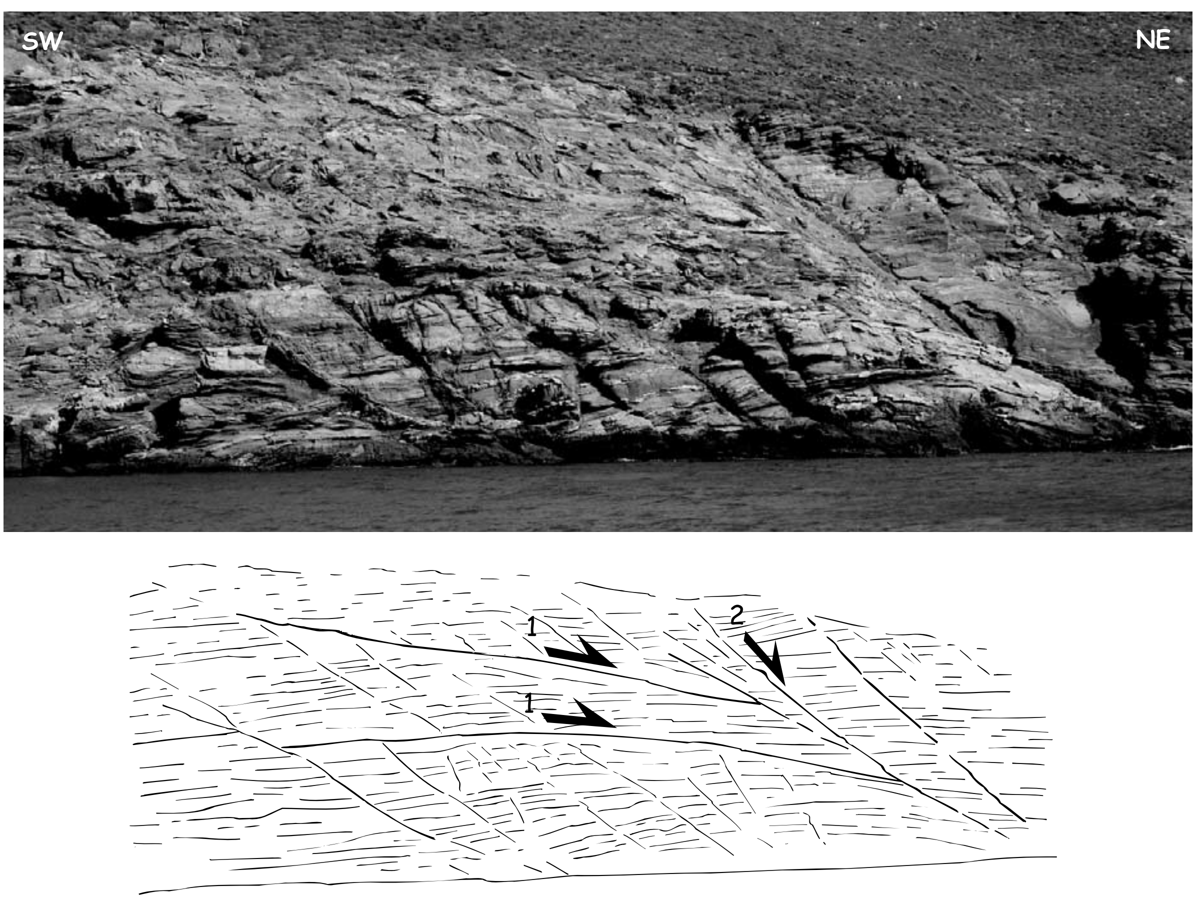

Figure 9

Table 1. Trends and Plunges of Axes of Stress Tensors Deduced From the Direct Inversion of Orientation and Striae of Faults[a]

Outcrop[b]	Lithology	Number of Fault Planes	σ_1[c]	σ_2[c]	σ_3[c]	$\phi = (\sigma_2 - \sigma_3)/(\sigma_1 - \sigma_3)$	Quality Estimator
Ormos Isternia	metapelites	15	350/83	144/06	234/03	0.44	B
Mali	metapelites	53	080/83	299/06	208/05	0.53	A
Planitis	metapelites	12	048/76	141/01	231/14	0.43	A
Kolimpithra (east)	metabasites	4	326/67	138/23	229/03	0.48	B
Kolimpithra (east)	metapelites	9	006/63	157/24	252/12	0.37	C
Kolimpithra (west)	metabasites	12	104/79	296/11	205/02	0.75	A
Kolimpithra (west)	metapelites	25	031/77	143/05	234/12	0.49	A
Kolimpithra (west)	breccia	6	149/69	290/17	024/13	0.46	C
Falatados	granite	6	305/27	068/48	198/30	0.36	B
Constriction (whole island)		21	292/25	085/62	197/11	0.66	B
Livada	granite	18	109/72	290/18	200/00	0.63	A
Livada	metapelites	15	109/62	295/28	203/02	0.70	A

[a]A quality estimator has been attributed to each numerical result on the basis of the number and variety of attitudes of faults and of an intra-algorithm estimator accounting for the mean deviation between the computed striations and shear stresses and the actual measured striations.
[b]Locations are given in Figure 1.
[c]The values of sigma correspond to two angles (in degrees), the first one being the trend of stress axis and the second one being its plunge.

4.2.3. Implication for the Initiation of Normal Faults

[56] The main implication of Andersonian's mechanics concerns the angle between σ_1 and conjugate fault planes. As already explained, this angle depends on the rheology of rocks undergoing deformation, the maximum angle expected in brittle crustal materials being 45°. In Tinos, this angle clearly depends on lithology. It is smaller in the metabasites than in the metapelites: the first ones are more competent than the second ones. Statistical analysis of dip angles of normal faults shows an ubiquitous plot of normal faults with a dip less than 45°, especially in metapelites whereas stress inversion as well as the widespread developed vein patterns unambiguously indicates a subvertical direction of compression. In order to make a precise comparison between outcrops with vertical σ_1 and those registering a moderate possible rotation of σ_1, the angles between normal faults and σ_1 have been plotted for the 161 fault planes of the nine outcrops. A global histogram of frequency of angles between fault planes and the principal stress axis is reported on Figure 10. Even if most faults create with an angle with σ_1 minor to 45°, the number of shallow-dipping faults is significant: 34 of them (that is 20% of the total) make an angle with σ_1 between 45 and 85° and 59 make an angle larger than 40°. The major part of the reactivated shear bands (NE dipping) are situated in Mali. Even if we consider the totality of shallow-dipping faults of Mali are inherited shear bands, we can consider that 60% of the planes making an angle greater than 45° with σ_1 correspond to newly formed shallow-dipping faults.

[57] One way to explain the formation of shallow-dipping planes is to consider that they formed with steep dips under a vertical compression and that they underwent a late rotation which caused the presently observed shallow dip. However, these shallow-dipping planes are closely associated (and coeval) with vertical veins (see above), so no rotation of structures can be advocated to explain shallow-dipping faults of Tinos.

[58] Most mechanical models propose a local rotation of principal stress orientations to account for the initiation of low-angle normal faults [*Spencer and Chase*, 1989; *Yin*, 1989; *Melosh*, 1990; *Parsons and Thompson*, 1993]. All models explain the rotation by unusual boundary or loading conditions. *Wills and Buck* [1997] tested these models by a simple Coulomb failure analysis. They concluded that the models predict low-angle fault development at the less favorable places for fault slip to occur and demonstrate that the strength and pore pressure required to initiate slip on such shallow-dipping planes are unrealistic. Again, a model of stress rotation cannot be considered in Tinos: The stress tensors deduced from inversion of fault slip data show a subvertical orientation of σ_1 in agreement with widespread development of subvertical extensional joints and crystallized veins. We thus identified "anticonjugate" normal fault systems in Tinos, the main compression axis being located in the obtuse angle of the system. No available mechanical model is satisfying in this case. Indeed, no model takes into account the possibility of the newly formation of brittle shallow-dipping planes together with the fact that the main principal stress axis σ_1 remains vertical. One way to explain field observations is to consider [after *Axen and Selverstone*, 1994] that the detachment is very weak until the later increments of deformation, most of the displacement being accommodated by ductile flow along shear bands and being relayed by cataclastic flow when approaching the brittle-ductile transition. Shallow-dipping planes could correspond to the later stages of

Figure 9. Illustrations of the chronology between steeply dipping and shallow-dipping normal faults. Steeply dipping faults always cut across shallow-dipping ones: shallow-dipping faults predate steeply dipping ones.

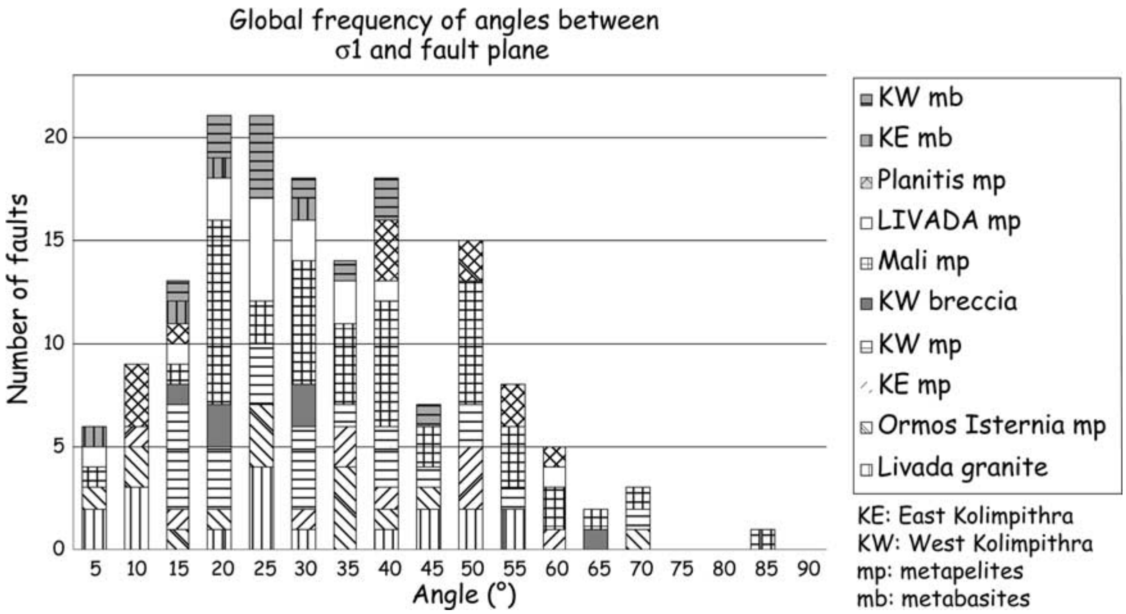

Figure 10. Number of faults versus the angle they make with the principal stress axe σ_1. The angles are divided into sequences of 5°. Each pattern is associated with an outcrop; 34 faults on 161 make an angle with σ_1 greater than 45°, which corresponds to the maximum angle predicted by the classical fracturing mechanics. It means 20% of faults do not seem to obey the laws of Andersonian's mechanics.

deformation and presumably did not accommodate a significant amount of extensional shear.

5. Discussion and Conclusion: Ductile to Brittle Transition and Progressive Localization of Deformation Along the Tinos Crustal Detachment

[59] Combined observations of ductile and brittle structures of the footwall of a major crustal detachment of Tinos, together with the results of other regional studies [e.g., *Jolivet et al.*, 2004], led us to conclude to the consistency of NE-SW extension during the extensional collapse of the Hellenides and the evolution of structures from ductile to brittle. The continuum of deformation is clearly demonstrated in Tinos during the complete way back of rocks to the surface.

[60] Two kinds of brittle normal faults have been identified in this study: shallow and steeply dipping fault planes. Some of shallow-dipping normal faults are interpreted as resulting from the "reactivation" of earlier ductile shear bands, in other words, as resulting from the ultimate localization of shear within precursory ductile or semibrittle shear bands. This assumption, supported by field observations, is in good agreement with the mechanical model of *Axen and Selverstone* [1994]. The model supposes slip of the Whipple detachment on preexisting weakness under low fluid pressure, high differential stress and steep principal stress axis. Other shallow-dipping faults have apparently newly formed through the metamorphic pile. Steeply dipping normal faults always cut across shallow-dipping ones: they are characteristic of the latest stage of localization.

[61] We propose a conceptual sketch of evolution of deformation from ductile toward brittle. A four-step scenario can be derived (Figure 11, right): (1) setting of early ductile structures, such as sheath folds or crenulation; initial localization of ductile deformation by formation of boudins; (2) localization of shear bands at the ends or in the neck between boudins (almost systematic localization of shear bands at the ends or in the necks between boudins confirm that rheological heterogeneity and boudinage is one more factor leading to the localization of shear zones and ultimately to the localization of faults); (3) brittle slip on preexisting shear bands and development of newly formed shallow-dipping faults under vertical shortening axis (slip occurs until the latest stages of brittle deformation, as pointed out by the fact that new shallow-dipping faults are coeval with vertical veins that correspond to a late stage of brittle deformation); and (4) final localization of brittle deformation with

Figure 11. Scenario of progressive localization of structures from ductile to brittle (right) at the scale of the island and (left) at the scale of the crust. See text for explanations.

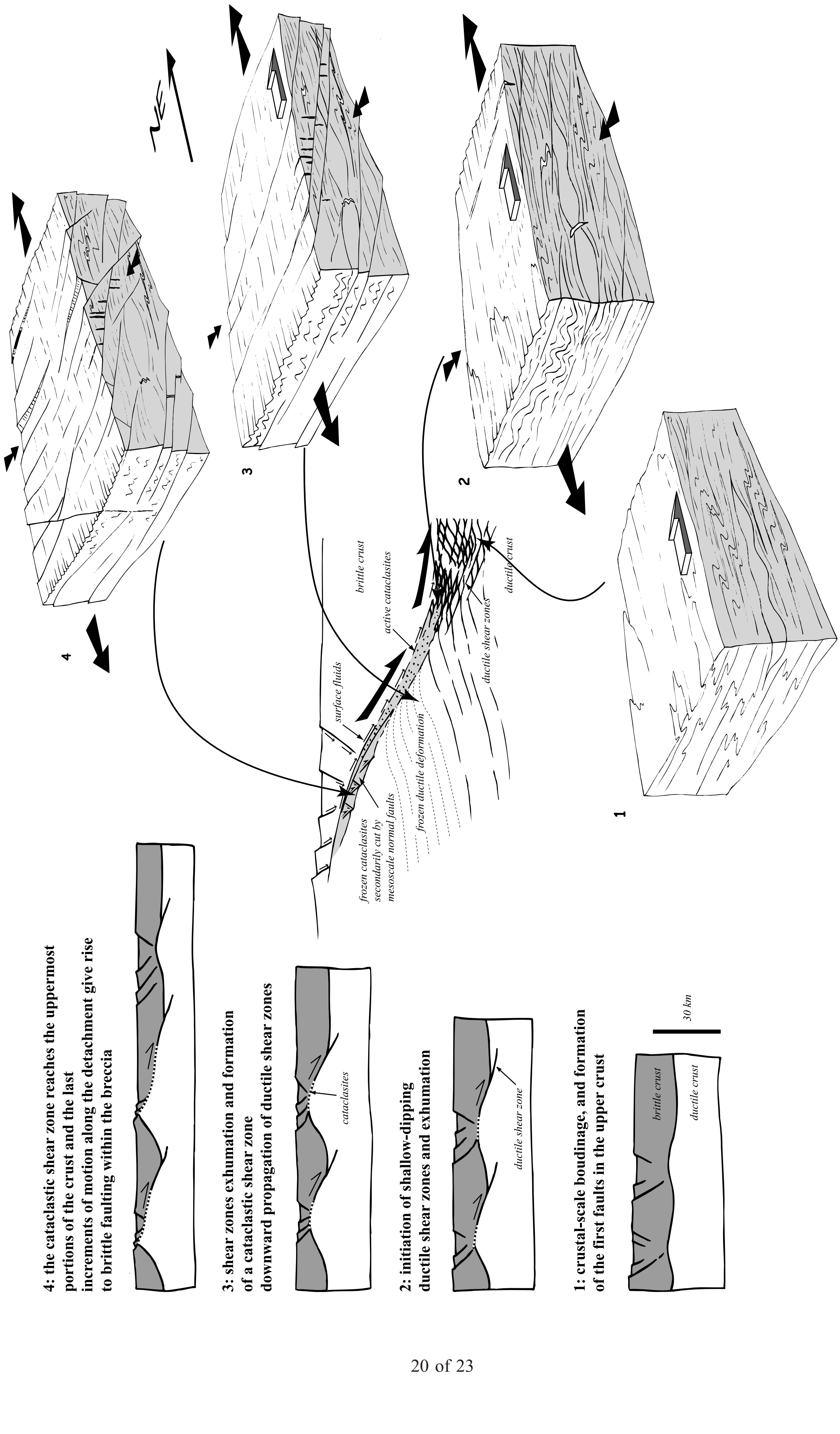
4: the cataclastic shear zone reaches the uppermost portions of the crust and the last increments of motion along the detachment give rise to brittle faulting within the breccia
3: shear zones exhumation and formation of a cataclastic shear zone downward propagation of ductile shear zones
cataclasites
2: initiation of shallow-dipping ductile shear zones and exhumation
ductile shear zone
1: crustal-scale boudinage, and formation of the first faults in the upper crust
brittle crust
ductile crust
30 km
frozen cataclasites secondarily cut by mesoscale normal faults
frozen ductile deformation
surface fluids
active cataclasites
brittle crust
ductile shear zones
ductile crust
NE
4
3
2
1

Figure 11

development of classical steeply dipping faults displaying conjugate patterns.

[62] Such a scenario, based on meter-scale field observations, can be discussed at the scale of the crust. *Jolivet et al.* [2004] observed crustal blocks displaying, in the Aegean Sea, a wavelength of several tens of kilometers. Extensional shear zones developed between the blocks. They proposed that metamorphic core complexes correspond to crustal-scale boudins. This model is derived from the megaboudinage concept of Davis [*Davis and Coney*, 1979; *Davis*, 1980] for the Basin and Range MCC. It further introduces the idea that boudinage is the first event that leads to the localization of shear zones and ultimately of faults when crossing the ductile to brittle transition. The progressive localization of strain in regions between boudins presumably led to stress concentration and higher strain rate. At the brittle-ductile transition, crustal-scale shear zones form in these regions of higher strain rate. The detachment of Tinos corresponds to the last step of evolution of one of these crustal-scale shear zones.

[63] The observation that the orientation and dip of late vertical veins do not change across the dome of foliation shows that doming is inherited from the ductile part of the deformation history (megaboudinage) and that the arch was frozen in the brittle field. Moreover if the foliation shows this clear arching the geometry of the detachment itself is more complex. Remnants of the upper units on the SW coast near Tinos city rest upon an older detachment below which blueschists and eclogites are well preserved and which was probably active in the Eocene as in the nearby island of Syros [*Trotet et al.*, 2001a, 2001b; *Jolivet et al.*, 2004]. The apparent shape of the detachment thus partly results from the megaboudinage during ductile extension but also from the interaction between the Oligo-Miocene and Eocene detachments.

[64] This study further reiterates the mechanical problem of initiation of newly formed shallow-dipping planes, when created under a vertical position of compression axis. The stress inversion of normal fault slip data and the statistical analysis of the angles between fault planes and the principal stress axis σ_1 reveal that 20% of faults of the island do not obey the classical fracturation mechanics.

[65] The consistency of tensors computed from normal fault sets all over the island, whatever the distance to the detachment and whatever the degree of asymmetry of the fault distribution, is in good agreement with their interpretation in terms of stress. The existence of conjugate faults, even where the system is asymmetric with a predominance of NE dipping planes probably related to the "reactivation" of earlier shear bands is compatible with the presence of vertical veins almost everywhere in the last brittle stages. Furthermore the observations of faults cutting through the cataclasites below the detachment suggest that, in the latest increments of strain, the cataclasite itself became stiff and acquired a frictional behavior.

[66] The vertical veins associated with the formation of shallow-dipping faults suggest that the detachment was not tilted after its formation and that it slipped with this shallow-dipping attitude. It is thus at high angle with the main compressive stress and might thus be interpreted as a weak fault or fault zone. The high content of micas of the matrix rocks (and probably of the fault gouge itself) could have favored this "weak" behavior. A similar situation is observed along the San Andreas Fault which is thus interpreted as a well lubricated, weak fault [*Zoback*, 1992; *Hickman and Zoback*, 2004].

[67] The amount of slip along the brittle-detachment sensu stricto is unknown. The total amount of displacement along the contact between the core complex and the upper unit is large, amounting to several tens of kilometers during the Oligo-Miocene extension [*Jolivet et al.*, 2004]. This amount is constrained by the metamorphic contrast between both units and much of it could have been accommodated by ductile deformation and cataclastic flow. The actual brittle slip would then only correspond to the very last increments of motion. This is only speculative but it would explain the overall geometry and kinematics with the most part of the detachment activity being achieved through ductile and cataclastic flow. The displacement along a shallow-dipping shear zone would thus no longer be problematic as it would be ductile during most of its life.

[68] The clear continuum of extension from ductile to brittle structures suggests that the detachment seen today is the last evolution of the ductile shear zone. Figure 11 (left) shows a cartoon of this progressive evolution at crustal scale. The first shear zones within the brittle-ductile transition form at the edge of crustal-scale boudins, and these shear zones are progressively exhumed together with the entire metamorphic dome. The main point is that the ductile shear zone forms in the conditions of the greenschist facies and progressively enters the brittle field during exhumation and is replaced by a thick zone of cataclasites. The cataclasites are localized where the crustal material has already been partially damaged by the formation of ductile and brittle-ductile shears bands at all scales. At this stage the crust presents the same vertical stratification of deformation mechanisms as described by *Sibson* [1983]. The cataclastic shear zone has the same dip as the original ductile shear zone and slip along this shallow-dipping plane is allowed by the weakness of the cataclastic material. During the last increments of strain the cataclasites are progressively abandoned while slip localizes along a narrower shear zone and ultimately to a single fault plane which accommodates the last, limited in amount, increment of slip while the extensional regime evolves toward more coaxial as suggested by conjugate patterns of late brittle normal faults. Outside the fault zone itself the stiffened material may be faulted in the same continuum. This evolution is facilitated by the circulation of surface-derived fluids down to the brittle-ductile transition as suggested by oxygene isotopes studies [*Famin et al.*, 2004a, 2004b]. Together with the high mica content of the rock, these fluids may have also allowed the brittle detachment to move (although of a likely limited amount) as a weak fault zone slipping under low shear stresses (i.e., high angle to the vertical $\sigma 1$ stress component).

[69] This study provides new insights into the way brittle crustal detachments may first initiate and further slip. It also questions available fault mechanics models and their potential to satisfactorily account for the initiation of small-scale to crustal-scale shallow-dipping normal faults under a vertical compression with evidence of neither structure nor stress rotation. The case study of the Tinos detachment finally draws attention on the possibility to partly solve the problem of the initiation of brittle flat detachments by considering that faulting is ultimately "prepared" by progressive localization along precursory crustal shear bands during exhumation while extensional deformation evolves from ductile to cataclastic then to brittle.

[70] **Acknowledgments.** The authors would like to thank G. H. Davis and an anonymous reviewer for their constructive comments which allowed the manuscript to be improved. Field studies were carried out within the framework of the program Dyeti (INSU/CNRS).

References

Agard, P., M. Fournier, and O. Lacombe (2003), Post-nappe brittle extension in the inner western Alps (Schistes Lustrés) following late ductile exhumation: A record of synextension block rotation?, *Terra Nova*, *15*, 306–314.

Altherr, R., H. Kreuzer, I. Wendt, H. Lenz, G. A. Wagner, J. Keller, W. Harre, and A. Höhndorf (1982), A late Oligocene/early Miocene high temperature belt in the Attic-Cycladic crystalline complex (SE Pelagonian, Greece), *Geol. Jahrb., Reihe E*, *23*, 97–164.

Anderson, E. M. (1951), *The Dynamics of Faulting*, 206 pp., Oliver and Boyd, Edinburgh, U.K.

Angelier, J. (1990), Inversion of field data in fault tectonics to obtain the regional stress-III. A new rapid direct inversion method by analytical means, *Geophys. J. Int.*, *103*, 363–376.

Angelier, J. (1994), Fault slip analysis and palaeostress reconstruction, in *Continental Deformation*, edited by P. L. Hancock, pp. 53–100, Elsevier, New York.

Armijo, R., H. Lyon-Caen, and D. Papanikolaou (1992), East-west extension and Holocene normal fault scarps in the Hellenic arc, *Geology*, *20*, 491–494.

Armijo, R., B. Meyer, G. C. P. King, A. Rigo, and D. Papanastassiou (1996), Quaternary evolution of the Corinth Rift and its implications for the late Cenozoic evolution of the Aegean, *Geophys. J. Int.*, *126*, 11–53.

Avigad, D., and Z. Garfunkel (1989), Low-angle faults above and below a blueschist belt: Tinos Island, Cyclades, Greece, *Terra Nova*, *1*, 182–187.

Avigad, D., G. Baer, and A. Heimann (1998), Block rotations and continental extension in the central Aegean Sea: Paleomagnetic and structural evidence from Tinos and Mykonos, *Earth Planet. Sci. Lett.*, *157*, 23–40.

Avigad, D., A. Ziv, and Z. Garfunkel (2001), Ductile and brittle shortening, extension-parallel folds and maintenance of crustal thickness in the central Aegean (Cyclades, Greece), *Tectonics*, *20*, 277–287.

Axen, G. J., and J. Selverstone (1994), Stress state and fluid-pressure level along the Whipple detachment fault, California, *Geology*, *22*, 835–838.

Bergerat, F. (1987), Stress field in the European platform at the time of Africa-Eurasia collision, *Tectonics*, *6*, 99–132.

Block, L., and L. Royden (1990), Core complex geometries and regional scale flow in the lower crust, *Tectonics*, *9*, 521–534.

Bott, M. H. P. (1959), The mechanisms of oblique slip faulting, *Geol. Mag.*, *96*, 109–117.

Brace, W. F., and D. L. Kohlstedt (1980), Limits on lithospheric stress imposed by laboratory experiments, *J. Geophys. Res.*, *85*, 6248–6252.

Bröcker, M. (1990), Blueschist-to-greenschist transition in metabasites from Tinos Island, Cyclade, Greece: Compositional control or fluid infiltration, *Lithos*, *25*, 25–39.

Bröcker, M., and L. Franz (1998), Rb-Sr isotope studies on Tinos Island (Cyclades, Greece): Additional time constraints for metamorphism, extent of infiltration-controlled overprinting and deformational activity, *Geol. Mag.*, *135*, 369–382.

Bröcker, M., H. Kreuzer, A. Matthews, and M. Okrusch (1993), $^{40}Ar/^{39}Ar$ and oxygen isotope studies of polymetamorphism from Tinos Island, Cycladic blueschist belt, Greece, *J. Metamorph. Geol.*, *11*, 223–240.

Bröcker, M., D. Bieling, B. Hacker, and P. Gans (2004), High-Si phengite records the time of greenschist facies overprinting: implications for models suggesting megadetachments in the Aegean Sea, *J. Metamorph. Geol.*, *22*, 427–442.

Brun, J. P., and J. Van Den Driessche (1994), Extensional gneiss domes and detachment fault systems: Structure and kinematics, *Bull. Soc. Geol. Fr.*, *165*, 519–530.

Brun, J. P., D. Sokoutis, and J. Van Den Driessche (1994), Analogue modeling of detachment fault systems and core complexes, *Geology*, *22*, 319–322.

Buck, W. R. (1988), Flexural rotation of normal faults, *Tectonics*, *7*, 959–973.

Coney, P. J., and T. A. Harms (1984), Cordilleran metamorphic core complexes: Cenozoic extensional relics of Mesozoic compression, *Geology*, *12*, 550–554.

Crider, J., and D. Peacock (2004), Initiation of brittle faults in the upper crust: A review of field observations, *J. Struct. Geol.*, *26*, 691–707.

Crittenden, M. D., Jr., P. J. Coney, and G. H. Davis (Eds.) (1980), *Cordilleran Metamorphic Core Complexes*, *Mem. Geol. Soc. Am.*, *153*, 490 pp.

Davis, G. A., and G. S. Lister (1988), Detachment faulting in continental extension; Perspectives from the southwestern U.S. Cordillera, in *Processes in Continental Lithospheric Deformation*, edited by S. P. J. Clark, *Spec. Pap. Geol. Soc. Am.*, *218*, 133–159.

Davis, G. H. (1980), Structural characteristics of metamorphic core complexes, southern Arizona, in *Cordilleran Metamorphic Core Complexes*, edited by M. D. Crittenden Jr., P. J. Coney, and G. H. Davis, *Mem. Geol. Soc. Am.*, *153*, 35–77.

Davis, G. H. (1983), Shear-zone model for the origin of metamorphic core complexes, *Geology*, *11*, 342–347.

Davis, G. H., and P. J. Coney (1979), Geologic development of the Cordilleran metamorphic core complexes, *Geology*, *7*, 120–124.

Davis, G. H., and J. J. Hardy (1981), The Eagle Pass detachment, southeastern Arizona: Product of mid-Miocene listric(?) normal faulting in the southern Basin and Range, *Geol. Soc. Am. Bull.*, *92*, 749–762.

Dixon, J., and G. Williams (1983), Reaction softening in mylonites from arnaboll thrust, Sutherland, *Scott. J. Geol.*, *19*, 157–168.

Famin, V. (2003), Incursion de fluides dans une zone de cisaillement ductile (Tinos, Cyclades, Grèce): Mécanismes de circulation et implications tectoniques, Ph.D. thesis, 296 pp., Univ. Pierre et Marie Curie, Paris.

Famin, V., S. Nakashima, L. Jolivet, and P. Philippot (2004a), Behaviour of metamorphic fluids inferred from Infrared microspectroscopy on natural fluid-inclusions: An example from Tinos Island (Greece), *Contrib. Mineral. Petrol.*, *146*, 736–749.

Famin, V., P. Philippot, L. Jolivet, and P. Agard (2004b), Evolution of hydrothermal regime along a crustal shear zone, Tinos Island, Greece, *Tectonics*, *23*, TC5004, doi:10.1029/2003TC001509.

Fitz Gerald, J. D., and H. Stünitz (1993), Deformaton of granitõuml;ds at low metamorphic grade: Reactions and grain size reduction, *Tectonophysics*, *221*, 269–297.

Flotté, N. (2003), Caractérisation structurale et cinématique d'un rift sur détachement: Le rift de Corinthe-Patras, Grèce, 197 pp., Univ. Paris-Sud XI, Paris.

Gautier, P., and J. P. Brun (1994a), Crustal-scale geometry and kinematics of late-orogenic extension in the central Aegean (Cyclades and Evvia Island), *Tectonophysics*, *238*, 399–424.

Gautier, P., and J. P. Brun (1994b), Ductile crust exhumation and extensional detachments in the central Aegean (Cyclades and Evvia islands), *Geodin. Acta*, *7*, 57–85.

Gautier, P., J. P. Brun, and L. Jolivet (1993), Structure and kinematics of upper Cenozoic extensional detachment on Naxos and Paros (Cyclades Islands, Greece), *Tectonics*, *12*, 1180–1194.

Gautier, P., J. P. Brun, R. Moriceau, D. Sokoutis, J. Martinod, and L. Jolivet (1999), Timing, kinematics, and cause of Aegean extension: A scenario based on a comparison with simple analogue experiments, *Tectonophysics*, *315*, 31–72.

Gueydan, F., Y. Leroy, and L. Jolivet (2001), Grain-size sensitive flow and shear stress enhancement at the brittle to ductile transition of the continental crust, *Int. J. Earth Sci.*, *90*, 181–196.

Gueydan, F., Y. M. Leroy, L. Jolivet, and P. Agard (2003), Analysis of continental midcrustal strain localization induced by microfracturing and reaction-softening, *J. Geophys. Res.*, *108*(B2), 2064, doi:10.1029/2001JB000611.

Hickman, S., and M. Zoback (2004), Stress orientations and magnitudes in the SAFOD pilot hole, *Geophys. Res. Lett.*, *31*, L15S12, doi:10.1029/2004GL020043.

Holm, D. K., J. W. Geissman, and B. Wernicke (1993), Tilt and rotation of the footwall of a major normal fault system: Paleomagnetism of the Black Mountains, Death Valley extended terrane, California, *Geol. Soc. Am. Bull.*, *105*, 1373–1387.

Jackson, J. A. (1987), Active normal faulting and continental extension, *Geol. Soc. Spec. Publ.*, *28*, 3–18.

Jackson, J. A., and N. J. White (1989), Normal faulting in the upper continental crust: Observations from regions of active extension, *J. Struct. Geol.*, *11*, 15–36.

Jiménez-Munt, I., R. Sabadini, A. Gardi, and G. Bianco (2003), Active deformation in the Mediterranean from Gibraltar to Anatolia inferred from numerical modeling and geodetic and seismological data,

J. Geophys. Res., *108*(B1), 2006, doi:10.1029/2001JB001544.
John, B. E., and D. A. Foster (1993), Structural and thermal constraints on the initiation angle of detachment faulting in the southern Basin and Range: The Chemehuevi Mountains case study, *Geol. Soc. Am. Bull.*, *105*, 1091–1108.
Jolivet, L., and C. Faccenna (2000), Mediterranean extension and the Africa-Eurasia collision, *Tectonics*, *19*, 1095–1106.
Jolivet, L., and M. Patriat (1999), Ductile extension and the formation of the Aegean Sea, in *The Mediterranean Basins: Tertiary Extensions Within the Alpine Orogen*, edited by B. Durand et al., *Geol. Soc. Spec. Publ.*, vol. 156, 427–456.
Jolivet, L., J. M. Daniel, C. Truffert, and B. Goffé (1994), Exhumation of deep crustal metamorphic rocks and crustal extension in back-arc regions, *Lithos*, *33*, 3–30.
Jolivet, L., C. Faccenna, B. Goffé, M. Mattei, F. Rossetti, C. Brunet, F. Storti, R. Funiciello, J. P. Cadet, and T. Parra (1998), Mid-crustal shear zones in post-orogenic extension: The northern Tyrrhenian Sea case, *J. Geophys. Res.*, *103*, 12,123–12,160.
Jolivet, L., V. Famin, C. Mehl, T. Parra, D. Avigad, and C. Aubourg (2004), Progressive strain localization, crustal-scale boudinage and extensional metamorphic domes in the Aegean Sea, in *Gneiss Domes in Orogen*, edited by D. L. Whitney, C. Teyssier, and C. S. Siddoway, *Spec. Pap. Geol. Soc. Am.*, *380*, 185–210.
Katzir, Y., A. Matthews, Z. Garfunkel, M. Schliestedt, and D. Avigad (1996), The tectono-metamorphic evolution of a dismembered ophiolite (Tinos, Cyclades, Greece), *Geol. Mag.*, *133*, 237–254.
King, G., and M. Ellis (1990), The origin of large local uplift in extensional regions, *Nature*, *348*, 689–693.
Kirby, S. H. (1985), Rock mechanics observations pertinent to the rheology of the continental lithosphere and the localization of strain along shear zones, *Tectonophysics*, *119*, 1–27.
Le Pichon, X., and J. Angelier (1981), The Aegean Sea, *Philos. Trans. R. Soc. Lond., Ser. A*, *300*, 357–372.
Le Pichon, X., N. Chamot-Rooke, and S. Lallemant (1995), Geodetic determination of the kinematics of central Greece with respect to Europe: Implications for eastern Mediterranean tectonics, *J. Geophys. Res.*, *100*, 12,675–12,690.
Letouzey, J. (1986), Cenozoic paleostress pattern in the Alpine foreland and structural interpretation in a platform basin, *Tectonophysics*, *132*, 215–231.
Lister, G. S., and G. A. Davis (1989), The origin of metamorphic core complexes and detachment faults formed during Tertiary continental extension in the northern Colorado River region, U.S.A., *J. Struct. Geol.*, *11*, 65–94.
Lister, G. S., G. Banga, and A. Feenstra (1984), Metamorphic core complexes of cordilleran type in the Cyclades, Aegean Sea, Greece, *Geology*, *12*, 221–225.
Livaccari, R. F., J. W. Geissman, and S. J. Reynolds (1993), Paleomagnetic evidence for large-magnitude, low-angle normal faulting in a metamorphic core complex, *Nature*, *361*, 56–59.
Livaccari, R. F., J. W. Geissman, and S. Reynolds (1995), Large-magnitude extensional deformation in the South Mountains metamorphic core complex, Arizona: Evaluation with paleomagnetism, *Geol. Soc. Am. Bull.*, *107*, 877–894.
Marquer, D., D. Gapais, and R. Capdevila (1985), Chemical changes and mylonitisation of a granodiorite within low-grade metamorphism (Aar Massif, central Alps), *Bull. Mineral.*, *108*, 209–221.
McClusky, S., et al. (2000), Global Positioning System constraints on plate kinematics and dynamics in the eastern Mediterranean and Caucasus, *J. Geophys. Res.*, *105*, 5695–5720.
Melidonis, M. G. (1980), The geology of Greece: The geological structure and mineral deposits of Tinos Island (Cyclades, Greece), *Rep. 13*, 1–80 pp., Inst. of Geol. and Miner. Explor., Athens.
Melosh, H. J. (1990), Mechanical basis for low-angle normal faulting in the Basin and Range province, *Nature*, *343*, 331–335.
Mercier, J. L., D. Sorel, and P. Vergely (1989), Extensional tectonic regimes in the Aegean basins during the Cenozoic, *Basin Res.*, *2*, 49–71.
Miller, E. L., P. B. Gans, and J. Garling (1983), The Snake River decollement: An exumed mid-Tertiary brittle-ductile transition, *Tectonics*, *2*, 239–263.
Mitra, G. (1978), Ductile deformation zones and mylonites: The mechanical processes involved in the deformation of crystalline basement rocks, *Am. J. Sci.*, *278*, 1057–1084.
Parra, T., O. Vidal, and L. Jolivet (2002), Relation between deformation and retrogression in blueschist metapelites of Tinos Island (Greece) evidenced by chlorite-mica local equilibria, *Lithos*, *63*, 41–66.
Parsons, T., and G. A. Thompson (1993), Does magmatism influence low-angle normal faulting?, *Geology*, *21*, 247–250.
Patzak, M., M. Okrusch, and H. Kreuzer (1994), The Akrotiri Unit of the island of Tinos, Cyclades, Greece: Witness to a lost terrane of late Cretaceous age, *Neues Jahrb. Geol. Paläontol. Abh.*, *194*, 211–252.
Reynolds, S., and G. Lister (1987), Structural aspects of fluid-rock interactions in detachment zones, *Geology*, *15*, 362–366.
Rietbrock, A., C. Tibéri, F. Scherbaum, and H. Lyon-Caen (1996), Seismic slip on a low angle normal fault in the Gulf of Corinth: Evidence from high resolution cluster analysis of microearthquakes, *Geophys. Res. Lett.*, *23*, 1817–1820.
Rigo, A., H. Lyon-Caen, R. Armijo, A. Deschamps, D. Hatzfeld, K. Makropoulos, P. Papadimitriou, and I. Kassaras (1996), A microseismicity study in the western part of the Gulf of Corinth (Greece): Implications for large-scale normal faulting mechanisms, *Geophys. J. Int.*, *126*, 663–688.
Ring, U., and P. W. Layer (2003), High-pressure metamorphism in the Aegean, eastern Mediterranean: Underplating and exhumation from the Late Cretaceous until the Miocene to Recent above the retreating Hellenic subduction zone, *Tectonics*, *22*(3), 1022, doi:10.1029/2001TC001350.
Sachpazi, M., C. Clément, M. Laigle, A. Hirn, and N. Roussos (2003), Rift structure, evolution, and earthquakes in the Gulf of Corinth, from reflection seismic images, *Earth Planet. Sci. Lett.*, *216*, 243–257.
Scott, R. J., and G. S. Lister (1992), Detachment faults: Evidence for a low-angle origin, *Geology*, *20*, 833–836.
Seyitoglu, G., and B. Scott (1991), Late Cenozoic crustal extension and basin formation in west Turkey, *Geol. Mag.*, *128*, 155–166.
Seyitoglu, G., and B. C. Scott (1996), The cause of N-S extensional tectonics in western Turkey: Tectonic escape vs. back-arc spreading vs. orogenic collapse, *J. Geodyn.*, *22*, 145–153.
Sibson, R. H. (1983), Continental fault structure and the shallow earthquake source, *J. Geol. Soc. London*, *140*, 741–767.
Sokoutis, D., J. P. Brun, J. V. D. Driessche, and S. Pavlides (1993), A major Oligo-Miocene detachment in southern Rhodope controlling north Aegean extension, *J. Geol. Soc. London*, *150*, 243–246.
Sorel, D. (2000), A Pleistocene and still-active detachment fault and the origin of the Corinth-Patras rift, Greece, *Geology*, *28*, 83–86.
Spencer, J. E., and C. G. Chase (1989), Role of crustal flexure in initiation of low-angle normal faults and implications for structural evolution of the Basin and Range province, *J. Geophys. Res.*, *94*, 1765–1775.
Stolz, J., M. Engi, and M. Rickli (1997), Tectonometamorphic evolution of SE Tinos, Cyclades, Greece, *Schweiz. Mineral. Petrogr. Mitt.*, *77*, 209–231.
Trotet, F., L. Jolivet, and O. Vidal (2001a), Tectono-metamorphic evolution of Syros and Sifnos islands (Cyclades, Greece), *Tectonophysics*, *338*, 179–206.
Trotet, F., O. Vidal, and L. Jolivet (2001b), Exhumation of Syros and Sifnos metamorphic rocks (Cyclades, Greece). New constraints on the P-T paths, *Eur. J. Mineral.*, *13*, 901–920.
Twiss, R. J., and J. R. Unruh (1998), Analysis of fault slip inversions: Do they constrain stress or strain rate?, *J. Geophys. Res.*, *103*, 12,205–12,222.
Wallace, R. E. (1951), Geometry of shearing stress and relation to faulting, *J. Geol.*, *59*, 118–130.
Wdowinski, S., and G. J. Axen (1992), Isostatic rebound due to tectonic denudation: A viscous flow model of a layered lithosphere, *Tectonics*, *11*, 303–315.
Weathers, M. S., J. M. Bird, R. F. Cooper, and D. L. Kohlstedt (1979), Differential stress determined from deformation-induced microstructures of the Moine Thrust Zone, *J. Geophys. Res.*, *84*, 7495–7509.
Wernicke, B. (1981), Low-angle normal faults in the Basin and Range province: Nappe tectonics in an extending orogen, *Nature*, *291*, 645–648.
Wernicke, B. (1992), Cenozoic extensional tectonics of the U.S. Cordillera, in *The Geology of North America*, vol. G3, *The Cordilleran Orogen: Conterminous U.S.*, edited by B. C. Burchfiel, P. W. Lipman, and M. L. Zoback, pp. 553–581, Geol. Soc. of Am., Boulder, Colo.
Wernicke, B. (1995), Low-angle normal faults and seismicity: A review, *J. Geophys. Res.*, *100*, 20,159–20,174.
Wernicke, B. P., and G. J. Axen (1988), On the role of isostasy in the evolution of normal fault systems, *Geology*, *16*, 848–851.
White, S. H., and R. J. Knipe (1978), Transformation- and reaction-enhanced ductility in rocks, *J. Geol. Soc. London*, *135*, 513–516.
Wibberly, C. (1999), Are feldspar-to-micas reactions necessarily reaction-softening process in fault zones?, *J. Struct. Geol.*, *21*, 1219–1227.
Wills, S., and W. R. Buck (1997), Stress-field rotation and rooted detachment faults: A Coulomb failure analysis, *J. Geophys. Res.*, *102*, 20,503–20,514.
Wintsch, R. P., R. Christoffersen, and A. K. Kronenberg (1995), Fluid-rock reaction weakening of fault zones, *J. Geophys. Res.*, *100*, 13,021–13,032.
Yin, A. (1989), Origin of regional, rooted low-angle normal faults: A mechanical model and its tectonic implications, *Tectonics*, *8*, 469–482.
Zoback, M. L. (1992), First- and second-order patterns of stress in the lithosphere: The World Stress Map Project, *J. Geophys. Res.*, *97*, 11,703–11,728.

L. Jolivet, O. Lacombe, and C. Mehl, Laboratoire de Tectonique, UMR 7072, Université Pierre et Marie Curie, T 46-00 E2, case 129, 4 place Jussieu, 75252 Paris Cedex 05, France. (caroline.mehl@lgs.jussieu.fr)